Thomas J. Vogl
Wolfgang Reith
Ernst J. Rummeny
Editors

Diagnostic and Interventional Radiology

Springer

Diagnostic and Interventional Radiology

Thomas J. Vogl
Wolfgang Reith
Ernst J. Rummeny
(Eds.)

Diagnostic and Interventional Radiology

Springer

Editors
Thomas J. Vogl
Institut für Diagnostische und Interventionelle Radiologie, Klinikum der Johann-Wolfgang Goethe-Universität, Frankfurt, Germany

Wolfgang Reith
Klinik für Diagnostische und Interventionelle Neuroradiologie, Universitätsklinikum des Saarlandes, Homburg/Saar, Germany

Ernst J. Rummeny
Institut für Radiologie, TU München Klinikum rechts der Isar, München, Germany

ISBN 978-3-662-44036-0 ISBN 978-3-662-44037-7 (eBook)
DOI 10.1007/978-3-662-44037-7

Library of Congress Control Number: 2016938818

Printed on acid-free paper

This Springer imprint is published by Springer Nature
The registered company is Springer-Verlag GmbH Berlin Heidelberg

Foreword

Modern diagnostic and interventional radiology are, more than other fields, subject to constant change. More than ever, as technical progress continually increases and the diagnostic and interventional therapeutic possibilities develop, radiologists and colleagues from other fields of medicine need to have a complete overview of the field of radiology. Unfortunately, there are not many books in this field that present the essentials of radiology at a specialist "state-of-the-art" level.

In this respect, the publisher of the present publication has accepted this challenge to create an up-to-date reference. It serves as a guide for beginners throughout their specialist training and provides an overview of the complete radiological field for more experienced practitioners.

The publisher and authors have succeeded in presenting the whole radiological field with today's standard in concise chapters, accompanied by more than 2,500 high-quality images. Early diagnosis and review, systematic approaches to image analysis, and common interventional procedures are included.

With regard to the increasing importance of imaging procedures and the rise in patient numbers in the fields of diagnostic and interventional radiology, the time available for structured specialist training is limited. For this reason, this book deserves wide distribution.

Prof. Dr. Maximilian Reiser
Head of the Department of Clinical Radiology at Ludwig Maximilian University of Munich

Preface

The fields of diagnostic and interventional radiology and neuroradiology are currently experiencing an enormous change. Technological and clinical innovations are major challenges to which the three disciplines are exposed. In addition, new forms of therapy challenge radiologists every day. Indicators for different diagnostic and interventional questions change annually, new techniques arise, and other techniques are replaced by more modern, less invasive or less stressful procedures. The continuing quality improvements cause the further standardization of diagnostic examinations and structuring of medical reports. The present book begins with the technical basics of imaging procedures. In the subsequent chapters clinical questions and examination-related aspects are juxtaposed.

Despite further specializations in the above-mentioned fields, it is crucial to define the specialist expertise required, the content of advanced training, and also to assemble the information for the prospective specialist. Indeed, the major challenge for publisher and authors is to focus on the essential information.

The increasingly restricted human and material resources combined with the higher performance rates require the focused use of the individual imaging methods according to clinical guidelines. It was initially attempted to adapt the usage of imaging procedures to the clinical protocols that are required for the radiological and clinical disciplines and questions.

In collaboration with the publisher Springer Science+Business we have structured the entire body of knowledge and summarized it in this book. Navigating this dynamic process and extracting the essential information has given us – the publisher and authors – much pleasure and we hope that the reader will get a taste of this enthusiasm in the numerous chapters that follow.

We have managed to prepare a compendium for prospective specialists primarily concerned with structured training and its implementation in daily practice. As this process is very dynamic, further work has to be done to optimize it.

As authors and publisher, we hope that there is a high demand for a structured systematic and clear presentation of the technology, indications, diagnostic criteria, and differential diagnosis, in addition to interventions in the areas of diagnostic and interventional radiology and neuroradiology.

We would like to thank all our colleagues who supported this book – both in the preliminary phase and during the preparation of the content. Moreover, we want to thank the representatives of Springer Science+Business and Corinna Schaefer, the editor, for their competent guidance and enormous commitment.

Thomas J. Vogl
Wolfgang Reith
Ernst J. Rummeny

Table of Contents

List of Contributors

Vogl, Thomas J., Prof. Dr. med.
Institut für Diagnostische und Interventionelle Radiologie
Klinikum der Johann-Wolfgang-Goethe-Universität
Theodor Stern Kai 7
60590 Frankfurt
t.vogl@em.uni-frankfurt.de

Reith, Wolfgang, Prof. Dr. med.
Klinik für Diagnostische und Interventionelle
Neuroradiologie
Universitätsklinikum des Saarlandes
66421 Homburg/Saar

Rummeny, Ernst J., Prof. Dr. med.
Institut für Radiologie
Klinikum rechts der Isar
Technische Universität München
Ismaninger Straße 22
81675 München

Balzer, Jörn O., Prof. Dr. med.
Chefarzt, Ärztlicher Direktor
Katholisches Klinikum Mainz
Klinik für Radiologie und Nuklearmedizin
St. Vincenz und Elisabeth Hospital
An der Goldgrube 11
55131 Mainz

Beer, Ambros, Prof. Dr. med.
Ärztlicher Direktor
Klinik für Nuklearmedizin
Universitätsklinikum Ulm
Albert-Einstein-Allee 23
89081 Ulm

Bodelle, Boris, Dr. med.
Institut für Diagnostische und Interventionelle Radiologie
Klinikum der Johann-Wolfgang-Goethe-Universität
Theodor-Stern-Kai 7
60590 Frankfurt

Brügel, Melanie, PD Dr. med.
Radiologie am Stiglmaierplatz
Nymphenburgerstr. 1
80335 München

Diebold, Thomas, Dr. med.
Radiologische Gemeinschaftspraxis
Schwerpunkt Senologische Diagnostik
Bad Homburg
Hessenring 64
61348 Bad Homburg

Dobritz, Martin, Dr. med.
Institut für Radiologie
Klinikum rechts der Isar
der Technischen Universität München
Ismaninger Straße 22
81675 München

Eiber, Matthias, Dr. med.
Institut für Radiologie
Klinikum rechts der Isar
der Technischen Universität München
Ismaninger Straße 22
81675 München

Engels, Hans-Peter, Dr. med.
Radiologie im Zentrum
Halderstraße 29
86150 Augsburg

Gaa, Jochen, Prof. Dr. med.
Institut für Radiologie
Klinikum rechts der Isar
der Technischen Universität München
Ismaninger Straße 22
81675 München

Hannig, Christian, Prof. Dr. med.
Institut für Radiologie
Klinikum rechts der Isar
der Technischen Universität München
Ismaninger Straße 22
81675 München

Hellerhoff, Paul, Dr. med.
Klinikum Dritter Orden
Abteilung Radiologie
Menzinger Straße 44
80638 München

Herzog, Christopher, Prof. Dr. med.
Radiologie München
Ärztehaus
Burgstraße 7
80331 München

Hillerer, Claudia, Dr. med.
Klinik für Nuklearmedizin
Klinikum rechts der Isar
der Technischen Universität München
Ismaninger Straße 22
81675 München

Holzapfel, Klaus, Dr. med.
Institut für Radiologie
Klinikum rechts der Isar
der Technischen Universität München
Ismaninger Straße 22
81675 München

Link, Thomas, Prof. Dr. med.
Department of Radiology
University of Southern California
1500 San Pablo Street
90033 Los Angeles, CA, USA

Marquart, Franz, Dr. med.
Internist – Endokrinologie
Lehrpaxis der Universität München
Isabellastraße 31
80796 München

Müller, Dirk, Dr. med.
Institut für Radiologie
Klinikum rechts der Isar
der Technischen Universität München
Ismaninger Straße 22
81675 München

Proschek, Petra, Dr. med.
MedKonsil Medizinisches Versorgungszentrum GmbH
Friedrichstraße 43
65185 Wiesbaden

Schmidt, Stefan, Dr. med.
Klinik für Nuklearmedizin
Klinikum rechts der Isar
der Technischen Universität München
Ismaninger Straße 22
81675 München

Stollfuss, Jens, PD Dr. med.
Abteilung für Radiologie
und Nuklearmedizin
Klinikum Memmingen
Bismarckstraße 23
87700 Memmingen

Dr. Ahmed Tawfik
Department of Diagnostic and Interventional Radiology
Mansoura University Hospital
Mansoura, Ägypten

Waldt, Simone, PD Dr. med.
Klinik für Radiologie und Neuroradiologie
Alfried Krupp Krankenhaus
Diagnostische Radiologie
Alfried-Krupp-Straße 21
45131 Essen

Wetter, Axel, Dr. med.
Rebenlaube 4
45133 Essen

Wuttge-Hannig, Anita, Dr. med.
Gemeinschaftspraxis Radiologie –
Strahlentherapie – Nuklearmedizin
Karlsplatz 3–5
80335 München

Zangos, Stephan, Prof. Dr. med.
Institut für Diagnostische und Interventionelle Radiologie
Universitätsklinikum Frankfurt
Goethe-Universität
Theodor-Stern-Kai 7
60590 Frankfurt

General Radiology

Physical Basics

W. Reith

T. J. Vogl, W. Reith, E. J. Rummeny (Eds.), *Diagnostic and Interventional Radiology,*
DOI 10.1007/978-3-662-44037-7_1, © Springer-Verlag Berlin Heidelberg 2016

1

1.1 Types of Radiation

Radiation refers to any free propagation of energy in space, although a distinction is made between particle radiation (corpuscular radiation) and wave radiation (electromagnetic radiation). Because quantum theory attributes properties to particles, electromagnetic wave radiation is also referred to as photon or quantum radiation. The energy of the radiation is measured in joules or electron volts. One joule is the energy required to raise a mass of 100 g through a height of 1 m. A charge (Q) can be accelerated by electric fields, whereby kinetic energy is recovered when a potential difference (U) passes through. An electron volt is the energy absorbed by an electron when a potential difference of 1 V is passed through. For the conversion, the following applies:

$$1\,\text{J corresponds to } 6.242 \times 10^{18} \text{ electron volts}$$

1.1.1 Particle Radiation

The component unit of particle radiation, the corpuscle, has a rest mass (m_0) and can carry a charge. Its energy is composed of the so-called rest energy (E_0) and kinetic energy (E_{kin}):

$$E = E_0 + E_{kin}$$

The rest energy is derived from the rest mass and the speed of light (c):

$$E_0 = m_0 \times c^2$$

1.1.2 Wave Radiation (Electromagnetic Radiation)

Electromagnetic waves consist of an electric and a magnetic field. In quantum theory, electromagnetic waves are attributed with properties of particles. These particles, photons, carry neither mass nor charge, but only the energy of the radiation.

Waves are described by their wavelength (λ), frequency (f) and amplitude (A). Wavelength and frequency are linked via the velocity of propagation (c):

$$C = \lambda \times f$$

Electromagnetic radiation always propagates at the speed of light. The energy of electromagnetic radiation is proportional to its frequency (f):

$$E = h \times f$$

h is Planck's constant. Electromagnetic waves also include visible light, infrared radiation, ultraviolet radiation, radio waves, X-rays, γ-rays and microwaves. They differ only in the frequency of the radiation and thus by their energy.

1.2 Structure of Matter and Radioactive Decay

1.2.1 Structure of Atoms

The atom is composed of protons, neutrons, and a shell of electrons. According to Rutherford's atomic model, atoms consist of a shell of negatively charged electrons and a positively charged nucleus. The electrons are bound to the nucleus via electromagnetic interactions. The nucleus consists of nucleons, the positively charged protons, and the uncharged neutrons. The nucleons are bound together by the nuclear force. In the range of the short distance from the atomic nucleus, this attractive force is much stronger than the repulsive electromagnetic force acting between the positively charged protons.

The atoms of a chemical element are characterised by the number of protons, which is known as the atomic number (Z) (Fig. 1.1). Atoms with the same number of protons, but a different number of neutrons (N) are referred to as isotopes of an element. An "atomic species", which is characterised by a certain number of protons and neutrons is referred to as a nuclide. The sum of protons and neutrons is called the mass number (A). An atom is electrically neutral if the number of electrons in the shell corresponds to the number of protons in the nucleus. If the number of shell electrons differs from the number of protons, the atom is electrically charged. It is no longer referred to as an atom, but rather as an ion. This condition is depicted by indicating the charge state e.g. Na^+, Cl^-, Fe^{2+}.

The theory of quantum mechanics developed at the beginning of the 20th century postulated that electrons can only move in shells of a certain energy (energy levels). The number of electrons per shell is thus restricted; the shells are arranged in order of increasing energy and referred to as K, L, M, N shells and so on. Their energy value corresponds to the energy required to completely separate the respective electron from the atom. Instead of leaving an atom (ionisation), an electron can pass to a shell of higher energy (excitation). The energy difference must be supplied to the electron, e.g. via radiation. If an excited electron returns to a shell of lower energy, the energy difference will be converted to characteristic radiation (X-rays) or an Auger electron in the case of a light atomic material. The emission of light is referred to as luminescence. By measuring the energy of the characteristic radiation (spectroscopy), the chemical element can be conclusively identified. The electron shell determines the electronic properties of an atom. Atoms with filled shells (e.g. the noble gases helium and neon) are chemically inert (Fig. 1.2).

The nucleus also has a shell structure, although like nucleons, the shell transitions are only possible with the absorption (nuclear excitation) or release (nuclear decay) of energy in the form of energy radiation.

In 1896, Becquerel discovered that a photographic plate becomes blackened upon exposure to uranium crystals. This led to the discovery of **radioactive decay**. In radioactive decay, the nucleus of a chemical element is spontaneously converted to the nucleus of another chemical element, thus emitting radiation. This property is referred to as radioactivity. Nuclides with this

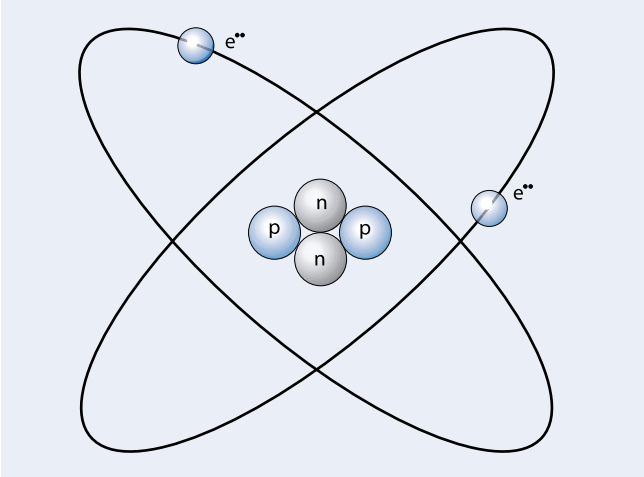

Fig. 1.1 Structure of an atom exemplified by ^{4}He (schematic diagram; *p* protons, *n* neutrons, e^- electrons)

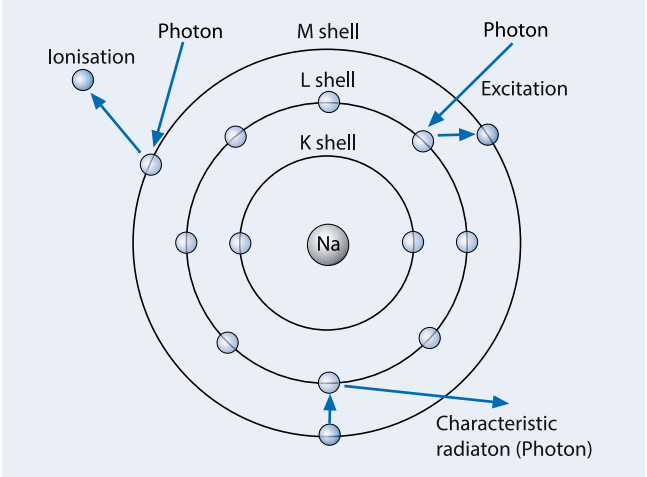

Fig. 1.2 The shell model exemplified by sodium. Schematic depiction of the excitation, ionisation and production of characteristic radiation (see text)

property are called radioactive nuclides. For most elements, stable and unstable (radioactive) isotopes can be distinguished. The newly created nucleus, which was created through radioactive decay, may itself be unstable, thus resulting in a chain of decay. The radioactive decay is classified according to the radiation emitted. If the same type of radiation is always released during the radioactive decay of an unstable nucleus, this is referred to as a pure emitter. For some radioactive nuclides, various types of decay occur (e.g. ^{64}Cu).

1.2.2 Forms of Radioactive Decay

α-Decay. In α-decay, α-radiation is emitted. By emitting a helium nucleus, element X is transformed into element Y. The mass number or atomic number is thus decreased by 2. The energy released is converted into kinetic energy of the helium nucleus.

β-Decay. In β-decay, β-radiation is emitted in the form of a β-particle (electron and positron). A distinction is therefore made between β^- and β^+-decay. In β^--decay, a neutron is converted into a proton after emitting an electron and an anti-neutrino. The atomic number of the element thus increases by 1. The anti-neutrino has no charge and only a negligible mass. However, it shares the kinetic energy released with the electron.
In β^+-decay, a proton is converted into a neutron after emitting a positron and a neutrino. Unlike β^--decay, the atomic number is only decreased by 1. The positron and neutrino share the energy released.

Shortly after it is formed, the positron combines with a shell electron. Two photons emerge (annihilation radiation), each with an energy of 0.511 MeV. When emitting a positron and a neutrino, an electron from the K shell can be integrated into the nucleus (electron, K-capture). The characteristic radiation is thus released. In β-decay and electron capture, the mass number remains the same.

γ-Decay. The γ-decay is not a real nuclear transformation because neither the mass number nor the atomic number changes. During this decay, an excited nucleus X+ (arising from α- or β-decay) is transferred to a state of lower energy following the emission of a photon (γ-quantum, therefore γ-radiation). If the core of the nuclide remains in the excited state for a long time, it is referred to as metastable. This is characterised by an "m" next to the mass number (e.g. ^{99m}Tc). They are pure γ-emitters.

1.2.3 The Law of Radioactive Decay

Radioactive decay is a stochastic process. For a single nucleus, only the decomposition probability per time interval or the average life can be specified.

The law of decay $N(t) = N_0 e^{-\lambda t}$ indicates the mean number of the initially existing cores (N_0) that are still present after time (t). Here, λ is the decay constant. The number disintegrations per second yield the activity of the radioactive isotope (unit = Becquerel = 1 disintegration/s). The half-life can be calculated from the mean lifespan of the radioactive isotope. The half-life is the time required for the radionuclide to be reduced to one-half its original activity.

Typical radionuclides used in medicine (along with their half-lives) include: ^{99m}Tc (6 h), ^{60}Co (5.3 years), ^{131}I (8 days), and ^{67}Ga (78 h).

1.3 Interaction of Radiation and Matter

1.3.1 General

In an interaction between radiation and matter, energy is transferred to atoms, which leads to excitation or ionisation. The interactions that lead to this are also called primary processes. Depending on whether the transmitted energy is sufficient for ionisation, it is called ionising or non-ionising radiation. Exam-

ples of ionising radiation are all kinds of corpuscular radiation in addition to X-rays, γ-rays and UV radiation. Non-ionising radiation includes visible light and heat radiation. Through collision with electrons, directly ionising radiation leads to excitation and ionisation. Indirectly ionising radiation is either absorbed or scattered by atoms. This leads to charged corpuscles, which, in turn, lead to excitation and ionisation. If indirectly ionising radiation strikes atoms, they can be absorbed or scattered by this and ultimately attenuated (Fig. 1.3).

There are **five forms of interaction** between photons and matter.

- The photoelectric effect
- The Compton effect
- Pair formation
- Classical scattering
- Nuclear reactions

The photoelectric effect, pair production and nuclear reaction are based on the absorption of a photon by an atom.

The Photoelectric Effect In the photoelectric effect, a photon strikes an electron shell and is absorbed. The total energy of the photon is transmitted to the shell electron. The electron, also referred to as a photoelectron, then moves away from the nuclear shell (ionisation) (Fig. 1.4). In the photoelectric effect, the energy of the photon is greater than the binding energy of the electron. The photoelectric effect predominantly takes place at the inner shells of the atom. The shell is re-filled by an electron from an outer shell, and characteristic radiation (or rarely an Auger electron) is emitted. If the radiation energy of the absorbed photons falls below the energy of a shell, an absorption edge occurs.

The Compton Effect In the Compton effect (Compton scattering), a photon releases a portion of its energy to a shell electron. Through the collision, the photon is deflected from its original direction, scattered, and continues to travel with a lower energy and frequency (Fig. 1.5).

Pair Formation For high radiation energies, so-called pair building occurs; a photon is absorbed by an atom (Fig. 1.6). In the field of the atomic nucleus, it is converted into an electron–positron pair. In the immediate vicinity of its point of origin, the positron combines with an orbital electron, thereby resulting in annihilation radiation with an energy > 1.022 MeV. The electrons formed in these interactions produce secondary electrons through further ionisation.

Classical Scattering In classical, coherent, or Rayleigh scattering, a photon strikes a shell electron, thereby changing its direction without transforming energy to the electron (Fig. 1.7). This means that there is no ionisation; the photon is simply scattered without any loss of energy.

Nuclear Reaction If an atom absorbs a photon with sufficient energy radiation, different nuclear reactions can occur. Of these, the emission of a proton or a neutron is the most important (Fig. 1.8).

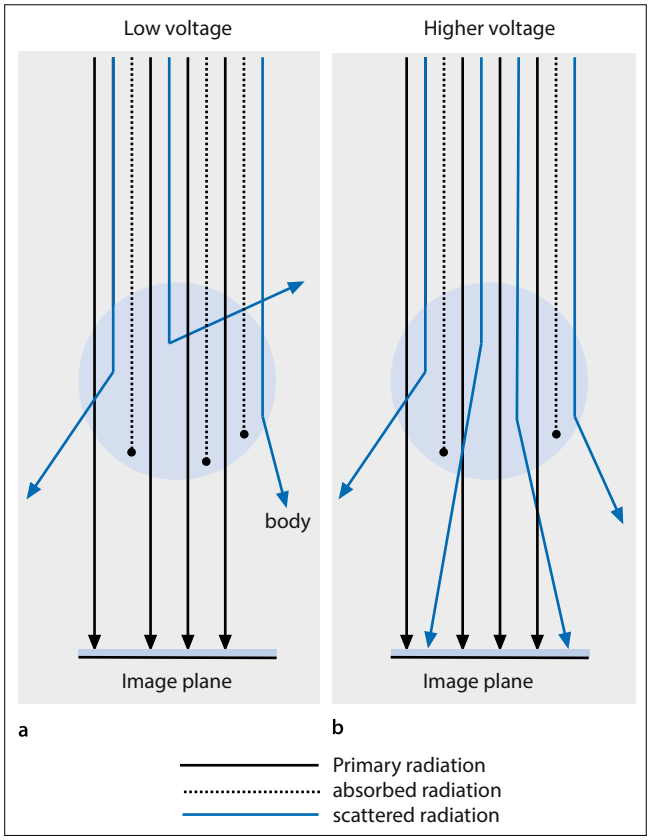

Fig. 1.3a,b Attenuation of the diagnostic X-rays for two different voltages, schematic depiction. **a** At low voltage, absorption predominates; the dispersion takes place in all directions, **b** At higher voltage, the absorption decreases, and the scattered radiation increases relatively; the radiation is scattered more in the direction of the primary radiation

1.3.2 X-Ray Radiation

In the interaction of radiation with matter, energy is transferred. Depending on how much energy is transferred to atoms, there will be either an excitation or ionisation. The interaction of radiation with matter is also referred to as the primary process.

If the energy transferred is sufficient to ionise atoms, it is called **ionising radiation**. If it is not sufficient, it is called **non-ionising radiation**. Ionising radiation includes all kinds of corpuscular radiation, such as X-rays, γ-rays and UV radiation (Fig. 1.9). Non-ionising radiation includes visible light and heat radiation.

Ionising radiation is often used in radiology and nuclear medicine and can be divided into **directly and indirectly ionising radiation**. Directly ionising radiation involves an electrically charged corpuscle, which can lead to excitation and ionisation (Table 1.1). Indirectly ionising radiation involves uncharged particles (neutrons), X-rays and γ-rays. They are either absorbed or scattered by atoms in matter. Which atoms are ionised depends on the energy of the ionising radiation. The frequency of the interaction of ionising radiation with matter primarily depends on the type of material: The greater the density of the matter (higher atomic number), the more frequently the interactions occur. There are several different types of interactions: the pho-

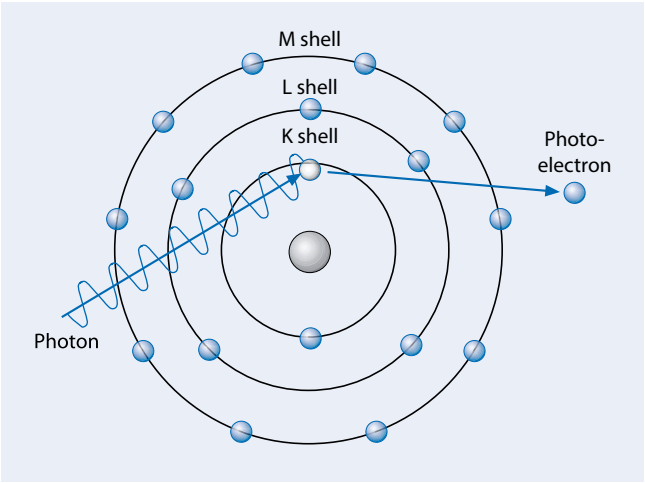

Fig. 1.4 Schematic representation of the photoelectric effect. Release of an electron from an inner shell by the complete absorption of a photon

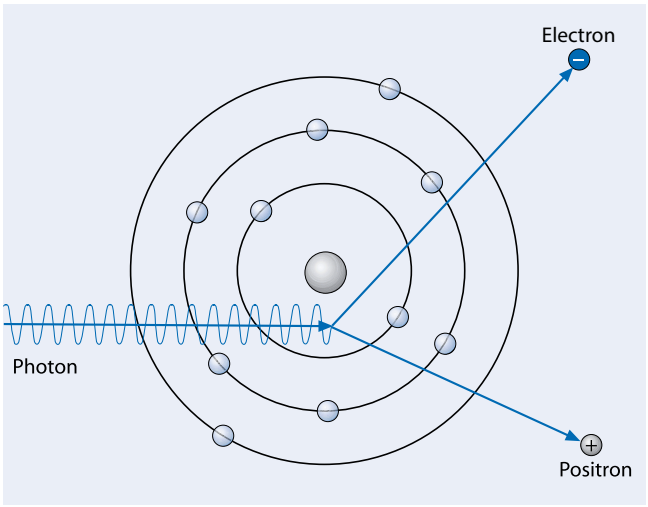

Fig. 1.6 Schematic representation of pair formation. Interaction with a nuclear field with one electron and one positron

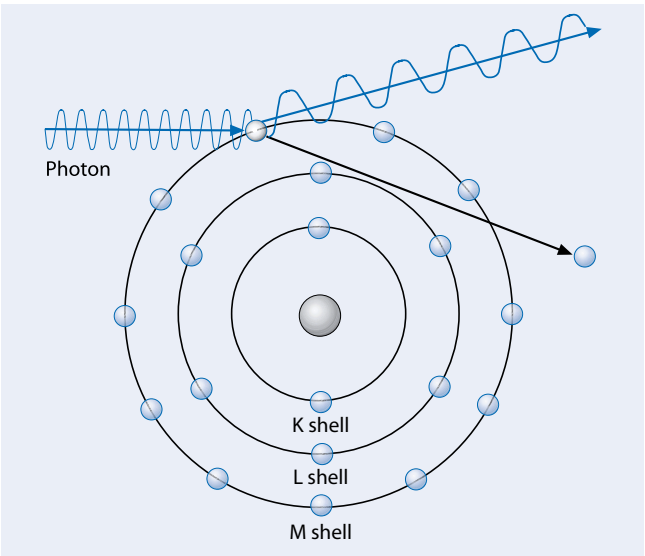

Fig. 1.5 Schematic depiction of the Compton effect. Release an electron from an outer shell by absorption of a photon; at the same time, a photon of lower energy is emitted at a different angle

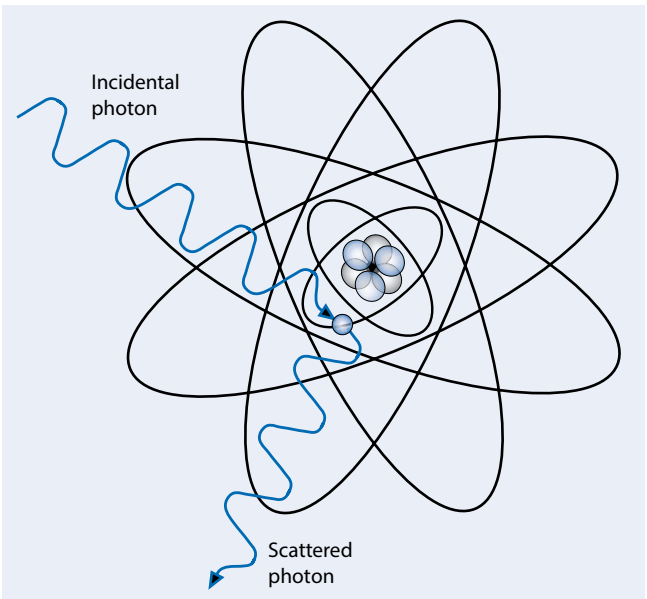

Fig. 1.7 Schematic depiction of classical scattering (see text)

toelectric effect, the Compton effect, pair formation, classical scattering and nuclear reaction (see above).

The effects of the interaction are: attenuation of the radiation (on which the different interactions have a different proportion, depending on the energy of radiation and material) and scattered radiation (Table 1.2). While the photo-absorption decreases with increasing energy, the Compton effect increases. For an additional increase in energy > 1.02 MeV pair formation occurs, and the Compton effect decreases. In X-ray radiation, attenuation is dependent on the voltage of the tube.

The attenuation of X-ray quanta in matter is determined by the so-called attenuation coefficient. The key factors for calculating the attenuation coefficients are the quantum energy, density, and atomic number of the attenuating material. The calculation of the total attenuation coefficient does not have any practical application because unlike the characteristic radiation, X-ray bremsstrahlung contains a relatively broad energetic quantum spectrum, which complicates the mathematical calculation. The radiation intensity decreases exponentially with increasing film thickness. The half-value layer indicates which slice thickness is halved by the radiation intensity. It should be noted that low-energy radiation is associated with a large mass attenuation coefficient and therefore leads to a high radiation dose.

Scattered radiation refers to the deflection of photons from their original direction in the case of Compton and classical scattering, which reduces the quality of radiographs. At energies around 100 keV, radiation in soft tissue is almost entirely absorbed by the Compton effect; to reduce this negative effect on the quality of the radiograph, a scattered radiation grid is placed in front of the film cassette in this range of energy.

In mammography, only low radiation energies of up to 30 keV are used for radiological investigation. Within this energy range, the proportion of the attenuation of the radiation is low so that good contrast among the different soft tissues can be obtained.

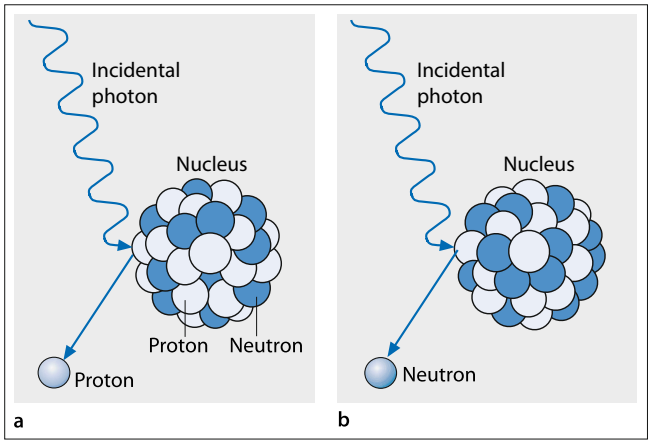

Fig. 1.8a,b Schematic depiction of the nuclear reaction. **a** Emission of a proton. **b** Emission of a neutron

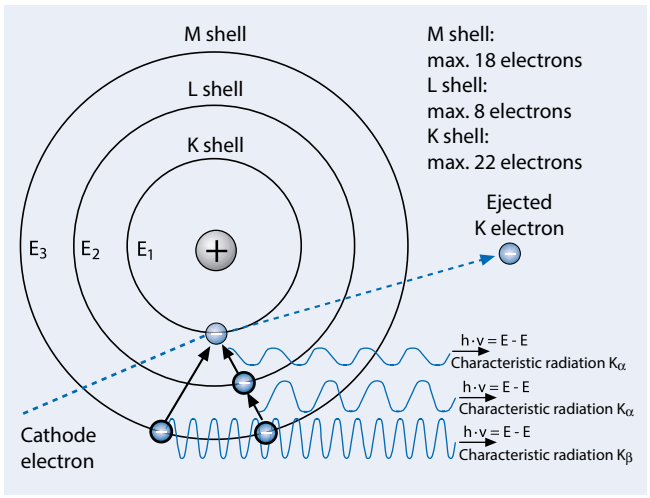

Fig. 1.9 Formation of the characteristic X-ray radiation (scheme). An electron from an anode atom is ejected from the K-shell by a cathode electron; the vacant place is occupied by an electron from either the outer shell or the overlying shell. If an electron jumps to a lower energy level, X-ray photons of a certain energy are released

Even the smallest calcifications can be visualised, although this requires a relatively high radiation dose. To reduce the negative influence of scattered radiation on image quality, an anti-scatter grid may be used.

1.4 Measurement of Radiation/Dosimetric Sizes

The energy dose is a measure of the amount of absorbed radiation and is related to the mass of absorbed radiation energy (Table 1.3). It is now considered the basic dosimetric parameter:

$$\text{Energy dose (D)} = \frac{\text{E (absorbed amount)}}{\text{M (bulk volume)}}$$

Because the dose in the body cannot be directly measured, it is calculated from the absorbed dose, which is generated in a dosimeter. The ion dose is usually measured in an air-filled ionisation chamber. Based on this, the energy dose of the material of interest can be determined. For radiation protection, the equivalent dose is determined.

Table 1.1 The most important corpuscles and their properties

Corpuscle	Charge	Mass compared with the electron	Energy at a range of 10 cm
Electron (β–)	–1	1	20 MeV
Positron (β+)	+1	1	20 MeV
Proton	+1	1.836	100 MeV
Neutron	0	1.839	–
α-particle (helium nucleus)	+2	7.294	600 MeV

The range of neutrons is not limited as with photons; only one exponential attenuation of the intensity takes place

Table 1.2 Attenuation of X-ray and photon radiation

Interaction with the electrons of the atomic shell	Absorption Classical scattering Compton scattering
Interaction with the nuclear field	Pairing formation > 1.02 MeV
Interaction with the nucleus	Nuclear reaction (very high photon energy)

Kerma Kerma stands for "kinetic energy released in matter" and is defined as the quotient of the kinetic energy of the secondary electrons produced in a volume and the mass of this volume.

Dose Rate The dose rate describes the amount of dose absorbed per unit of time. It corresponds to the quotient of the dose (ion energy, dose equivalent, or kerma) and the duration of exposure. It describes the irradiated dose per unit of time. This unit is determined by the dose (terms: Coulomb/kg/s: ion dose rate, Gray/s: absorbed dose rate, kerma rate, or Sievert/s: equivalent dose rate).

1.4.1 Measured Quantities in Nuclear Medicine

The activity of a radioactive substance follows the law of exponential decay. The activity indicates the number of decays per second. The unit is the Becquerel (Bq). One Bq is one disintegration per second. In nuclear medicine, the dosage of radioactive substances is based on the weight of the patient. A pre-determined amount of activity must therefore be prepared to examine the patient.

Using the specific activity, i.e. the number of decays per mass of absorbed substrate (unit Bq/kg), the desired activity can be calculated for the patient.

The physical half-life of the isotope used, the route of administration and bio-kinetics are crucial for the radiation dose.

The biological half-life refers to the time required for half of the activity of the isotope administered to be eliminated. From the physical and biological half-life, the effective half-life can be calculated, which is decisive for the patient's radiation dose.

1.4.2 Detection of Radiation

Radioactivity cannot be directly perceived; it is detected indirectly via so-called detectors, which respond reproducibly to irradiation (Table 1.4).

Ionisation Chamber An ionisation chamber is a gas-filled chamber containing two electrodes between which a voltage is applied. The absorbed dose can be calculated from the charge released.

Pocket Dosimeter For radiation protection, pocket dosimeters are used to monitor individuals. A pocket dosimeter consists of two electrodes, which enclose a gas-filled cavity. The electrons are charged before use. Incidental radiation ionises the gas molecules in the measuring volume, and the charge generated thus leads to a discharge of the electrodes. The degree of discharge is proportional to the dose.

Geiger–Müller Counter The Geiger-Müller counter is constructed like an ionisation chamber, but has a higher voltage. An electrode avalanche results in an amplification of the measuring pulse so that the particles can be counted. The activity can be determined from the number of pulses. By introducing material between the radiation source and the counter tube, the range of the radiation can be estimated. The type of radiation can thus be readily determined.

Because of their short range, α-particles are fully absorbed by a sheet of paper. For β-radiation, much more material is required (e.g. aluminium plates). γ-radiation is only slightly attenuated.

Film/Badge Dosimeter Film dosimetry is particularly important for the radiation monitoring of personnel in radiation businesses. Photographic emulsions and thus also X-ray films are blackened by the radiation. By determining the film density, the dose can be measured. Because there is usually a non-linear relationship between the blackening and the dose, the dose must be determined by using another dosimeter, e.g. an ionisation chamber. By comparing with a density curve, the dose can be determined for the measured blackening. Every 4 weeks, authorised measuring points evaluate the films of individuals exposed to radiation. Written documentation of the measurement results is submitted to the radiation safety officer; this is kept for 30 years.
In the badge dosimeter, dose measurement is combined with the determination of the radiation quality. The film cassette, which is made of pressed resin, is divided into five fields. One field does not have a cover; the other four fields are covered with metal filters. The uncovered area is blackened by low-energy radiation, while the filtered fields are blackened with increasing radiation energy. Conclusions can thus be drawn about the quality of the radiation. Film badges should be worn visibly at chest height under radiation protection clothing. The lower radiation detection limit is 0.2 mSv.

Thermoluminescence Detector The thermoluminescence detector consists of certain ionic crystals. Certain substances absorb energy upon irradiation; upon exposure to heat, this is re-emitted as light and can be measured. The light is then used as an indirect measurement dosimeter.

Finger Dosimeter Finger dosimeters are used to determine partial body doses at the hands of individuals working with X-rays, β-rays or γ-rays. The dose is within the range of 0.4 to 100 mSv.

Table 1.3 Important dosimetric quantities

Dosimetric quantity	S.I. unit
Ion dose (I)	Coulomb/kg (C/kg)
Energy dose (D)	Gray (Gy)
Kerma (K)	Gray
Equivalent dose (H)	Sievert (Sv)
Effective dose equivalent (H_{eff})	Sievert

Table 1.4 Overview of radiation detectors and their applications

Detector	Measuring principle	Preferred application
Ionisation chamber	Ionisation of gases and liquids	Radiotherapy: dose measurement
Pocket dosimeter	Ionisation of gas	Radiation protection
Geiger–Müller counter	Detection by the induction of charge avalanches	Nuclear medicine: measurement of activity
X-ray film, film dosimeters	Film blackening	Radiotherapy: radiation protection dosimetry
Thermoluminescence detector (TLD)	Excitation and storage of electrons in crystals	Radiotherapy: radiation protection dosimetry
Scintillation counter	Generation of photons by collisions in crystals	Nuclear medicine: detection of nuclear decay in patients
Iron sulphate dosimeter	Conversion of Fe^{2+} to Fe^{3+}	Radiotherapy: determination of the absolute dose
Water calorimeter	Heating of water	Radiotherapy: determination of the absolute dose

For photons, the energy range is between 15 and 3 MeV. For electrons, it is > 1 MeV. A thermoluminescence detector is covered by a 1-mm-thick copper filter. With such a detector, it is possible to identify the quality of the radiation. Ring dosimeter must be sterilised at low temperatures (maximum 60°C).

Scintillation Counter In the crystal of the scintillation detector, absorbed radiation emits photons, which can be detected by means of a photo-multiplier found behind the crystal. Scintillation detectors are used in nuclear medicine for the location-sensitive measurement of activity.

Radiation Biology and Radiation Protection

W. Reith

T. J. Vogl, W. Reith, E. J. Rummeny (Eds.), *Diagnostic and Interventional Radiology*,
DOI 10.1007/978-3-662-44037-7_2,

2.1 The Effects of Radiation on Biological Tissue

Modern radiotherapy and radiology would be unimaginable without knowledge of the fundamental effects of ionising radiation. All radiologists must be aware of the dangers and risks of the uncritical application of X-rays to diagnosis; this ensures the safety of both the patients and the radiologist. Because of CT and interventional radiological procedures, the patient and the physician are subjected to increased exposure to radiation. Knowledge of radio-biological principles and the use of ionising radiation is necessary.

Upon entering material or the body, ionising radiation loses part of its energy because of absorption. Energy transfer occurs via excitation and ionisation (primary processes). In biological tissue, only the absorbed radiation energy is effective; this can lead to cell damage. Biomolecules can be modified through chemical and biological processes (secondary processes). The effect of ionising radiation can be divided into phases. The changes in biomolecules are caused by the direct or indirect transfer of radiation energy to biomolecules (direct or indirect radiation effect).

Energy absorbed by the tissue can lead to ionisation, excitation of the molecule, and the generation of heat. The ionisation of water molecules leads to H_2O^+ and a free electron; in subsequent reactions, H and OH radicals are generated. Hydrated electrons also arise. The reaction products directly attack biomolecules and react with oxygen to generate peroxide radicals, which can further attack biomolecules.

Biochemical reactions can modify biomolecules. Changes in the nucleic acids of DNA lead to genetic damage. Changes to other biomolecules (e.g. proteins or lipids) may damage somatic cells or embryos (somatic and teratogenic radiation damage).

The direct effects of radiation can lead to primary damage of the cell. The cell can also be indirectly damaged by the free radicals generated (radiation effects).

2.1.1 Phases of the Effects of Radiation

In biological tissues, the effects of radiation proceed in four stages. The physical phase corresponds to the energy absorption in the tissue, which leads to ionisation, molecular excitation, and the generation of heat. These effects usually take place within 10–60 s.

Physical/Clinical Phase. This phase entails primary damage to the cell through the reaction of the excited or ionised atoms or molecules with other molecules. This produces free radicals – mainly water radicals. The formation and subsequent reaction of free radicals is completed approximately 1 ms after exposure to radiation.

The Biochemical Phase. This phase entails many chemical and biochemical processes. These include hydroxylation and decarboxylation as well as redox reactions. Organic molecules can be modified in the process. This may take place over seconds or years. In this phase, enzymatic reactions and bio-molecular repair processes are at the forefront.

The Biological Phase. The biological phase includes the effects of the physical and chemical processes. These processes disturb vital functions at the biological substrate, which can lead to cell death. At the same time, latent or manifest damage can occur, which can lead to both cell death and mutations. DNA damage is particularly severe (see below) because it contains all the relevant cellular information. This phase may persist over years or decades.

2.1.2 Radiation Damage to the Cell

Radiobiological studies of cells have significantly contributed to the understanding of the effects of ionising radiation on normal or tumour tissue. The effect of radiation concerns each individual cell, but it is modified by the cell structure. Inhibition of cell proliferation and cell death are the most serious and desired effects of radiation in tumour tissue.

Ionising radiation damages biological structures in a dose-dependent manner. The consequences of the damage manifest after a period of latency in which cellular and organic damage occurs.

Upon exposure to ionising radiation, hereditary factors or functional portions of DNA are damaged (mutation).

Each proliferating cell undergoes a cycle that can be divided into **mitosis and inter-mitosis**. During mitosis (M phase), cell division takes place. The inter-mitotic phase can be further subdivided into the G1 phase, the S phase, and the G2 phase.

In the **G1 phase**, cytoplasm, cell organelles, enzymes, and DNA components are produced to prepare for DNA synthesis. In the S phase, the DNA is replicated. The chromosomes now have two chromatids (diploid of chromosomes) (Fig. 2.1).

In the **G2 phase**, proteins and RNA are synthesised in preparation for mitosis. Depending on the cell type, the mitotic phase can last between 8 and 20 h.

The G1 phase, however, can last between hours and days. Proliferating cells can exit the cell cycle and enter a resting phase (G0). From the G0 phase, the cells can either re-enter the G1 phase or differentiate and eventually die. Studies have shown that cells in the various phases of the cycle have different sensitivities to radiation.

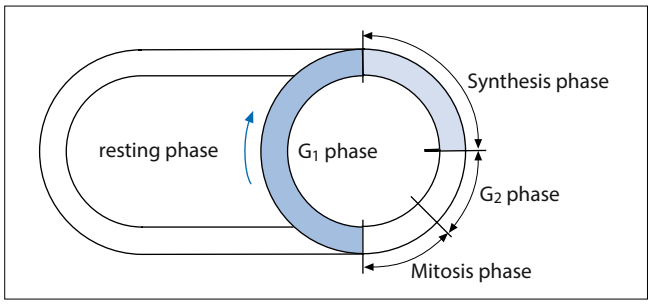

Fig. 2.1 Generation cycle of the cells. G1 phase = growth phase of the cells; G0 Phase = resting phase of the cells

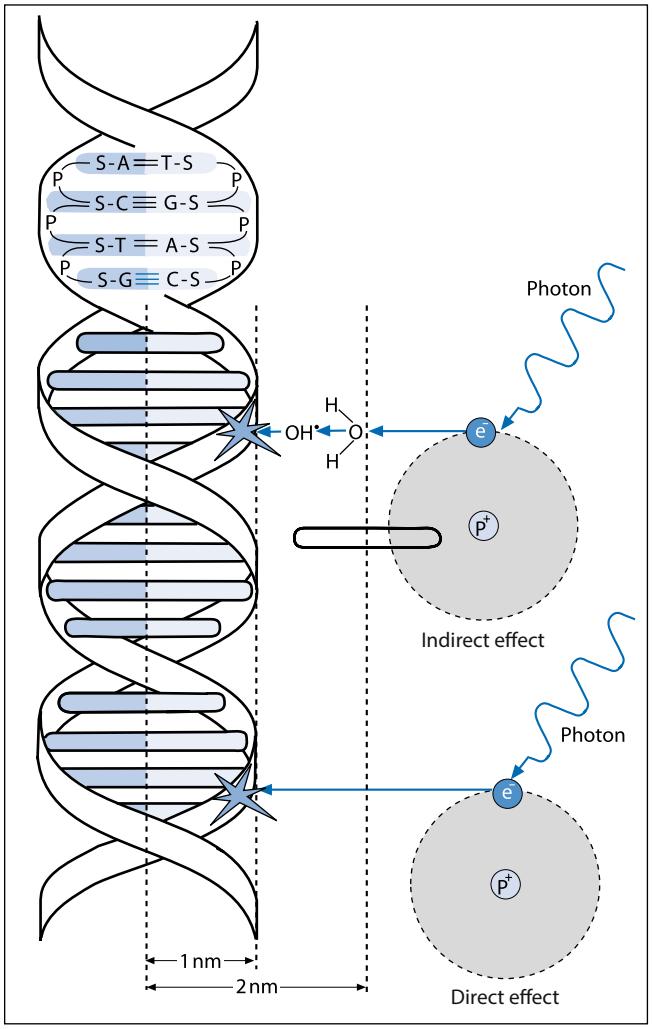

Fig. 2.2 Direct and indirect radiation effects can lead to changes in molecules

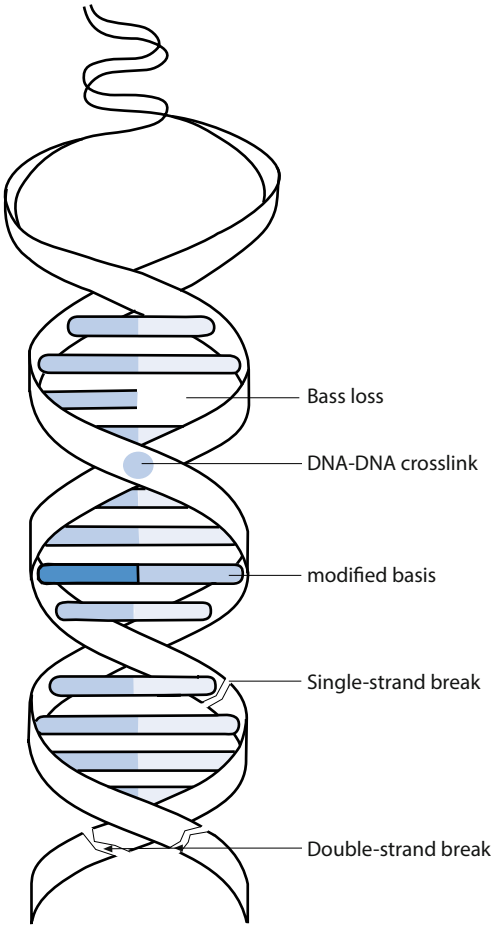

Fig. 2.3 Various types of DNA damage are caused by ionising radiation

Cells in the M phase are the most sensitive to radiation, followed by cells in the G2 phase and the S phase. Cells in the later stages of the S phase are highly resistant to radiation. Cells in the long G1 phase are also relatively resistant to radiation. The initial effects of radiation include temporary partial synchronisation of the cycle as well as a decrease in the rate of mitosis. The cell cycle is extended. After some time, surviving cells re-enter the radio-sensitive cell-cycle phases and are once again confronted with radiation.

The Effects of Radiation on Cellular Components

DNA damage has a particularly adverse effect on cells. The following types of DNA damage can occur as a result of the direct or indirect effects of radiation (Figs. 2.2 and 2.3)

- Single-strand break
- Double-strand break
- DNA cross-linking with intra-or intermolecular connections (crosslinks)
- Damage to bases whereby chemical modification or loss of bases can occur.
- Multiple damage, in which several types of DNA damage occur at once (bulky lesion).

Repair Mechanisms

Cellular systems can either completely or partially repair damage caused by radiation. Following exposure to radiation, repairs are performed within minutes to days. Single-strand breaks and damaged bases, for example, can be repaired by excising the damaged section.

Double-strand breaks can also be repaired or rendered harmless. Multiple damages can also be eliminated through various repair mechanisms. **Apoptosis** (programmed cell death) is an important repair system for eliminating irreparable cell damage.

The Consequences of Radiation Damage

Mutations can occur as a result of the direct and indirect effects of radiation as well as faulty repairs. Mutations are irreversible damage to genetic information. There are gene or point mutations, chromosomal mutations, and genomic mutations. In **point mutations** changes to a nucleotide occur, e.g. the loss as a base (deletion), the replacement of one base by another (transition and transversion), or the reversal of the order of the bases (inversion).

In **chromosomal mutations**, the structure of the chromosome is altered (i.e. deletion, duplication, translation, or inversion). One or both arms of the chromosome can be affected. Ring chromosomes or dicentric chromosomes may also be formed.

The detection of these changes in lymphocytes provides an indication of the radiation dose received (chromosome aberration analysis).

Genomic mutations entail changes to the number of chromosomes, e.g. monosomy or trisomy.

Mutations do not always result in clinical changes; they may remain silent, but can also lead to the degeneration or death of the cell.

2.1.3 The Acute Effects of Radiation on the Human Body

Acute effects of radiation effects can manifest up to 90 days after exposure. Tissues with a high cell turnover as well as the vascular system are predominantly affected. Rapidly proliferating and thus early-reacting tissues have a hierarchical organisation proliferation; radiation leads to the loss of stem cells, which rapidly manifests as a deficiency of functioning cells in these tissues. This ultimately leads to functional limitations.

In the vascular system, the capillaries are vasodilated and venules are contracted, thereby resulting in hyperaemia (erythema) and increased vascular permeability (oedema).

"**Acute radiation syndrome**" refers to a variety of symptoms that occur after extended partial or whole-body exposure to radiation. The distension of radiation syndrome depends on the duration and the intensity of the exposure.

Acute radiation syndrome usually proceeds in three phases:

- The prodromal phase is characterised by headaches, nausea, and vomiting. The higher the dose, the sooner the symptoms arise.
- In the latency phase, the affected individual is largely asymptomatic.
- In the main phase, radiation damage is manifested.

A dose of up to 2 Gy leads to fatigue and impaired concentration. From 7 Gy onward, the dose is lethal. The median lethal dose is 3–4 Gy (LD 50, i.e. 50% of the exposed persons die within 30 days).

2.1.4 The Chronic Effects of Radiation

Chronic effects of radiation occur from 90 days after exposure to radiation. Tissue with a low cell turnover, connective tissue, and the vascular system are all affected. Because of the slow turnover of cells, these tissues have a high repair capacity. In these tissues, the consequences of losing stem cells are not as serious. Radiation therapists fear the chronic effects of radiation because they are irreversible, partly progressive, and are difficult to treat.

2.1.5 Local Effects of Radiation

The Haematopoietic System. The bone marrow is very sensitive to radiation; the pluripotent stem cells are particularly sensitive. A single dose of irradiation of 3–4 Gy reduced the number of stem cells by approximately 90%. Stem cells can migrate from the periphery or from unradiated areas of bone marrow.

The Gastrointestinal Tract. The small intestine is the most sensitive to radiation; death of the epithelial cells leads to radiation enteritis. Symptoms include malabsorption and bloody diarrhoea as well as the loss of fluid and electrolytes. Radiation proctitis may occur in the colon.

Liver. If the liver is exposed to > 30 Gy of radiation, this may result in radiation hepatitis with the gradual occlusion of the central vein. Clinically, this manifests as an increase in liver enzymes, jaundice, hepatomegaly, and ascites.

Kidney. The kidneys are relatively resistant to radiation. However, high exposure to radiation can lead to radiation nephropathy with tubular atrophy and interstitial fibrosis, which manifests about 6 months after exposure to radiation. Radiation-induced hypertension may even occur 10 years after exposure to radiation.

The Lungs. Following exposure to 20–30 Gy of radiation, acute radiation pneumonitis may manifest after 4–8 weeks. This is clinically similar to an atypical viral pneumonia (cough, dyspnoea), but may also be asymptomatic. Pulmonary fibrosis is another chronic effect of radiation.

Circulatory System. As a result of the acute effects of radiation, long-term ECG changes such as pericardial effusion and pericarditis may occur. The changes that occur depend on the size of the vessel. Large vessels rarely experience acute or chronic radiation damage. Chronic effects of radiation appear relatively late in the arteriolar and capillary bed, but are nevertheless of vital importance. Exposure to radiation leads to the obliteration of the vascular bed in the arterioles and capillaries. Veins, however, are relatively resistant to radiation.

Nervous System. In the CNS, three radiation-induced effects can be described:

- Early changes that can occur within hours in the case of very high doses. Radiogenic oedema occurs because of a disturbance of the blood–brain barrier; this is referred to as radiation encephalitis or myelitis.
- An "early delayed reaction" occurs within 6 months of radiation. This can lead to sub-acute encephalitis, myelitis, or leukoencephalopathy. Reversible paraesthesia can also occur.
- "Late delayed reactions" occur after several months or years. This can result in radionecrosis, which is often difficult to differentiate from a tumour recurrence.

The peripheral nervous system is relatively resistant to radiation. However, delayed reactions can include paralysis.

The Skin. One of the most common side effects of radiotherapy is acute radiodermatitis. It manifested after a cumulative dose of 16–20 Gy or individual doses of 2 Gy. Depending on the dose,

erythema, oedema, dry desquamation, hair loss, epitheliolysis, haemorrhaging, and/or necrosis may appear. The severity can be mitigated through targeted skin care.
Chronic effects of radiation include atrophy of skin appendages, pigment changes, telangiectasia, epidermal atrophy, hypopigmentation, dyskeratosis, and ulcerations.

The Eyes. The lens is the organ most sensitive to radiation. Even at doses of about 10 Gy, radiation cataracts with a latency of months to years can develop. This can, however, be treated through cataract surgery and the insertion of a plastic lens. Acute keratoconjunctivitis may occur, which can regress to the end of the radiation. Radiation keratitis may lead to opacification or an ulcer of the cornea. Impairment of the lacrimal gland can lead to conjunctivitis sicca.

The Gonads. The gonads are among the most radiation-sensitive organs. In particular, the gonads of children should be protected from ionising radiation because these are approximately 10 times more sensitive to radiation than those of adults. Radiation can lead to failure of germ cell production, endocrine disorders, and genetic damage to germ cells.
In the **male gonads**, genetic changes can occur in the early stages of spermatogenesis. The sperm are relatively resistant to radiation. The threshold dose for radiation of the male gonads is 0.2 Gy.

The **female gonads**, namely the primary oocytes, are the most sensitive to radiation during the late stage of oogenesis. The secondary oocytes are less sensitive to radiation. Infertility can occur following exposure to higher doses. Amenorrhoea can result from doses as low as 1–2 Gy. The threshold dose for the most sensitive ovarian cells is 2–6 Gy.

Prenatal Radiation Damage. In blastogenesis (up to the 10th day of development), the all-or-nothing law applies. Radiation with a dose > 0.05 Sv can either lead to the death of the embryo or have no effect on normal development. Organ malformations occur during organogenesis, especially of the CNS (2nd–8th week of development). Neurological deficits or growth disorders can occur during foetogenesis (9th week of development until birth).

2.1.6 Carcinogenesis

Along with genetic damage, a malignant transformation of cells caused by mutations resulting from ionising radiation, a carcinogenic effect, is one of the stochastic effects of radiation. This means that there is no threshold dose. Even very small doses can lead to leukaemia, breast cancer, skin cancer, or thyroid cancer. For solid tumours, the average time to clinical manifestation is 20 years. For leukaemia, this is 5–10 years.

2.2 The Dangers of X-Rays

Statements are based on statistical calculations and are therefore only estimates of probability. If the body is exposed to X-ray radiation (electromagnetic wave), a small part of the energy of the X-rays is transferred to the body. In principle, all cellular substances could be damaged. Damage to the DNA of somatic cells can lead to cancer. 99.9% of DNA damage can be removed via repair mechanisms (see above). Haematopoietic bone marrow, the colon, female breast, the stomach, and the lung are all highly radiosensitive. The bladder, liver, oesophagus, and thyroid are moderately radiosensitive, while the skin, bone surface, and muscles are only slightly radiosensitive. Exposure to X-rays thus depends on the level of radiation dose as well as the site of radiation. Therefore, when estimating the dose, critical organs are more heavily weighted. A comparable effective dose is calculated, which is given in millisieverts per year (mSv/a). Cosmic rays, terrestrial radiation, natural radon inhalation, and absorption of natural radioactive substances can lead to a radiation dose of approximately 2.4 mSv/a. As a result of the Chernobyl disaster, the average radiation dose in Germany in 1990 was 0.025 mSv/a. Watching colour TV for 100 h (from a distance of 3 m) corresponds to 0.01 mSv/a, 100 h in front of a monitor (at a distance of 0.5 m) corresponds to 0.12 mSv/a, a 10-h flight corresponds to 0.1 mSv/a, and an increase in cosmic radiation exposure at 2,000 m above sea level corresponds to 0.6 mSv/a (the additional exposure given is based on the year). In contrast, a one-time X-ray investigation leads to an additional effective dose of:

- X-ray (▶ Chap. 3)
  - The skull: 0.03 to 0.1 mSv
  - The thorax: 0.02 to 0.08 mSv
  - The abdominal cavity: 0.6 to 1.2 mSv
  - The cervical spine: 2.0 mSv
  - The thoracic spine: 0.5 to 0.8 mSv
  - The lumbar spine: 0.8 to 1.8 mSv
  - The pelvis: 0.5 to 1.0 mSv
- CT (▶ Chap. 4):
  - The skull: 2.0 mSv
  - The thorax: 6 to 10 mSv
  - The abdominal cavity: 10 to 25 mSv
- Cardiac DSA: 10 mSv
- Thoracic fluoroscopy: 1.5 mSv

The risk of dying from radiation-induced cancer following a single X-ray examination is:

- 1 in 100,000 for X-ray examinations of the lungs and skull (the same risk as dying as a result of being struck by lightning within the next 10 years)
- 1 in 40,000 X-ray examinations of the thoracic spine and female breast (the same risk as being involved in a fatal traffic accident within the next 3 months)
- 1 in 10,000 for a CT of the head (the same risk as being involved in a fatal traffic accident within the next year)
- 1 in 2,000 for a CT of the spine (the same risk as being involved in a fatal traffic accident within 5 years)
- 1 in 1,000 for thoracic CT or angiography (the same risk as being involved in a fatal traffic accident within 10 years)

It can take many years for radiation-induced cancer to manifest. In this dose range, it can take up to 15 years for leukaemia and 40 years for other forms of cancer.

2.2.1 Radiation Exposure/Radiation Protection

In medicine, a substantial portion of the radiation exposure is a result of CT (30%) (► Chap. 4). In addition to strict indication, the dose can be reduced through the following measures:

- Reducing the energy (mA) to the minimum required value. This does, however, lead to increased noise.
- Increasing the pitch factor (ratio of the table feed to the slice thickness). Accelerating the table feed by 50% for constant nominal slice thickness is associated with a dose reduction of 33%. However, the effective slice thickness is increased by 50%.
- Precisely determining the area of examination. Once started, a spiral cannot be stopped.
- Storing raw data for possible reconstructions.

In Germany, one in four deaths is cancer related. This corresponds to a risk of 25%. A single X-ray examination of the lungs increases the risk to 25.001%. Changes in lifestyle can either reduce or increase the risk by 5%.

Each X-ray examination ultimately poses an incalculable risk. Therefore, X-ray examinations should only be performed when indicated (see below).

2.3 Radiation Protection and Quality Assurance in X-Ray Diagnostics

The German X-ray regulations (§ 16) require the implementation of quality assurance in X-ray diagnostics. The radiation protection supervisor (German X-ray regulations § 13) provides guidance in X-ray-related matters. The radiation protection supervisor provides support and is the operator in the radiology clinic. The radiation protection supervisor must neither possess expert knowledge nor personally supervise the use of radioactive materials or the operation of facilities.

2.3.1 Radiation Protection Officer (German X-Ray Regulations § 13)

The radiation protection supervisor appoints the radiation protection officer in writing. The radiation protection officer supervises the use of radioactive materials or the operation of radiation equipment and is obliged to follow the rules. The radiation protection officer must have proof of qualifications. The X-ray regulation stipulates that if the radiation protection officer is absent, a deputy must be appointed. Separate organisational departments with X-ray equipment must have their own radiation protection officer and deputy. The relevant state labour inspectorate must be notified in writing of the appointment of the radiation safety officer and the proof of expertise.

The radiation safety officer is only responsible for the obligations prescribed in the context of his/her internal area of responsibility (German X-ray regulations § 14). The radiation safety officer shall immediately notify the radiation protection supervisor of any and all deficiencies that affect radiation protection. The radiation protection supervisor must promptly notify the radiation safety officer of any administrative measures relating to his/her duties.

Using the appropriate measures, the radiation protection officer shall ensure that no humans are exposed to unnecessary radiation (German X-ray regulations § 15), that any exposure to radiation is kept as low as possible, that the appropriate safety regulations are adhered to, and that decisions on design approval are observed.

2.3.2 Obligation to Maintain Records of X-Ray Examinations (German X-Ray Regulations § 28)

Before the start of each X-ray examination or treatment, the patient must be asked about any previous applications of ionising radiation. This must be recorded. Appropriate entries shall be made in the X-ray records.

Female patients must be asked if they are pregnant. The aim of the survey is to avoid multiple investigations. The result of the survey shall be recorded. The records must include the time, the type of application, the body part that was treated or investigated, and the information used to determine the personal dose. The records shall be presented to the competent authorities upon request. The patients examined should be informed about the radiographic and fluoroscopic data on request.

2.3.3 Storage Requirements (German X-Ray Regulations § 28 and 35)

Records of X-ray treatments (radiation therapy) must be kept for 30 years after the last treatment. Records of X-ray examinations (including films) must be retained for 10 years after the last treatment. For patients younger than 18 years the records must be retained for 10 years after the 18th year of life. Records of measurements of the personal dose of persons who reside in the control region are kept for 30 years.

Radiographs remain the property of the institute in which the examination was performed.

2.3.4 Instruction (German X-Ray Regulations § 36)

Individuals working in the control area who use X-rays should be informed in advance about the working methods, the potential hazards, and the protective measures.

2.3.5 Radiation Protection Areas (Radiation Protection Ordinance § 57–60)

In the Radiation Protection Ordinance, protection areas have been defined:

- Prohibited area
- Control area
- Operational monitoring area
- External operational monitoring area

Prohibited Area

The prohibited area is a region with a dose rate that exceeds 3 MJ/kg/h (0.3 REM/h). The prohibited area must be marked as follows: **Prohibited area, no access**. Limited access is only allowed with special permission.

Controlled Area (German X-Ray Regulations § 19)

A stay in the controlled area is recommended if there is a possibility that a person might absorb more than 6 mSv per calendar year from whole body exposure. Access is limited to workers older than 18 years, trainees, and patients being examined. The controlled area is optional in the case of a possible radiation dose of 6 mSv per year (or organ doses > 45 mSv for the eye lens or > 150 mSv for the skin, hands, underarms, feet, or ankles). For occupationally exposed persons for whom the controlled area is prescribed, the condition does not change as a result of wearing protective clothing.

Operational Monitoring Area (German X-Ray Regulations § 19)

The operational monitoring area includes the rooms adjacent to the control area in which a body dose of > 1 mSv is achieved per calendar year in the case of permanent residence (or organ doses > 15 mSv for the eye lens or > 50 mSv for the skin, hands, underarms, feet, or ankles). The stay is allowed without time limit.

2.3.6 Quality Assurance in X-Ray Diagnostics (German X-Ray Regulations § 16)

For diagnostic X-ray equipment, acceptance testing shall be performed by the manufacturer or supplier before commissioning and after each modification of the device. In the acceptance test, all functional parameters of the system are reviewed, especially tube voltage, dose efficiency, switching functions, attenuation factors, centring of the useful beam and acquisition with the specimen.

At regular intervals – at least monthly – the operator is obligated to perform a consistency test with a test specimen and compare this with the original image. If there are differences in image quality compared with the original image, the operator shall determine the cause and rectify it. The results of the acceptance and constancy tests shall be made available to dental and medical authorities for examination.

The objective of the quality assurance measures is to achieve adequate image quality consistent with the requirements of medical science. With the customised X-ray examination, the diagnostic examination should be performed with radiation exposure that is as low as is reasonably justifiable. The regular constancy tests should lead to improvements in image quality and a reduction of radiation exposure and costs.

Acceptance Testing

For a new installation, an acceptance test verifies that the X-ray facilities are in an optimal condition and comply with legal obligations. The acceptance test is performed during commissioning and in the case of operational changes that might affect image quality or radiation protection. For smaller changes to the device (i.e. in the context of a repair or replacement) partial acceptance testing is sufficient. In accordance with the medical products law, acceptance testing does not apply to devices with the CE mark. However, the manufacturer and the supplier shall carry out acceptance testing that satisfies the product liability requirements.

2.3.7 Extracts from the German X-Ray Regulations

§ 31 Categories of Occupationally Exposed Persons

For the purposes of control and occupational health, individuals who are exposed to occupational radiation through activities covered by this regulation are assigned to the following categories:

(1) Occupationally exposed persons in category B:

Individuals who are exposed to occupational radiation exposure that can lead to an effective dose of > 6 mSv per calendar year or organ doses > 45 mSv for the eye lens or > 150 mSv for the skin, hands, underarms, feet, and ankles.

(2) Occupationally exposed persons in category B:

Individuals who are exposed to occupational radiation exposure that can lead to an effective dose of > 1 mSv per calendar year or organ doses > 15 mSv for the eye lens or > 50 mSv for the skin, hands, underarms, feet, and ankles.

§ 31a Dose Limits for Occupational Radiation Exposure

(1) For occupationally exposed persons, the effective dose should not exceed the limit of 20 mSv in a calendar year. In individual cases, the competent authority may allow an effective dose of 50 mSv for 1 year, although for 5 consecutive years, 100 mSv cannot be exceeded.

(2) For occupationally exposed individuals, the organ dose cannot exceed the following values:

- For the eye lens, the limit of 150 mSv
- For the skin, hands, forearms, feet and ankles, the limit of 500 mSv
- For the gonads, the uterus, and the red bone marrow, the limit of 50 mSv
- For the thyroid gland and the bone surface, the limit of 300 mSv
- For the colon, lung, stomach, bladder, breast, liver, oesophagus, other organs or tissues in accordance with Appendix 3, footnote 1, unless specified in point 3, the limit of 150 mSv

§ 31b Career Dose

The cumulative effective dose of occupationally exposed persons may not exceed the limit of 400 mSv. In accordance with § 41

para. 1 sentence 1, and upon consultation with a physician, the competent authority may allow a further occupational radiation exposure if it does not exceed an effective dose of 10 mSv in a calendar year and if the occupationally exposed person provides written consent.

§ 19 Radiation Protection Areas

(1) For activities requiring approval covered by these regulations, radiation protection areas are to be established in accordance with sentence 2. Depending on the amount of radiation exposure, a distinction is made between monitoring areas and control areas:

1. Monitoring areas are operational areas that do not belong to the control area in which individuals can be exposed to an effective dose > 1 mSv per calendar year or organ doses > 15 mSv for the eye lens or > 50 mSv for the skin, hands, underarms, feet, and ankles.
2. Controlled areas are areas in which individuals can be exposed to an effective dose > 6 mSv per calendar year or organ doses > 45 mSv for the eye lens or > 150 mSv for the skin, hands, underarms, feet, and ankles.

(2) Controlled areas must be delimited and labelled during times of operation. The labelling shall be clearly visible and contain at least the words "No Entry – X-ray"; it must also be present during standby mode.

(3) Local doses originating from other sources can be included in the definition of the boundaries of the control area and the monitoring area.

(4) The competent authority may order that other areas are to be treated as control areas or monitoring areas if this is necessary to protect individuals or the general public.

(5) The areas referred to in paragraphs 1 and 4 shall only apply as radiation protection areas when the radiator is turned on.

(6) In accordance with § 5, paragraph 1, the operation of portable X-ray equipment or interference radiator, a controlled area as referred to in para. 1, sentence 2, no. 2 shall be identified and delineated so that non-participating individuals do not inadvertently enter. If non-participating individuals can be excluded from inadvertently entering the controlled area, the delineation is not required.

§ 23 Justifiable Indication

(1) In the practice of medicine or dentistry, X-ray radiation may only be applied directly to the individual if a justifiable indication has been made in accordance with § 24, para. 1 no. 1 or 2. The justifying indication requires a statement that the health benefits of human use outweigh the risk of radiation. Other methods with comparable health benefits that are associated with no or less exposure to radiation are taken into account in the assessment. In accordance with sentence 1, a justifying indication shall also be made in the event of a request from a referring physician. The justifying indication may only be made if the physician issuing the justifying indication can personally examine the patient on site except in cases of application referred to in § 3 para. 4. § 28a remains unaffected.

(2) Prior to the application and if necessary, in cooperation with the referring physician, the physician issuing the justifying indication shall apply the currently available medical knowledge in order to prevent any unnecessary exposure to radiation. Patients must be asked about previous medical uses of ionising radiation relevant to the intended application.

(3) Prior to the application of X-rays in medicine or dentistry, the practising physician must ask women of childbearing potential about existing or potential pregnancy. If necessary, this may be done in collaboration with the referring physician. In the case of pregnancy or potential pregnancy, the urgency of the application should be considered.

Conventional Diagnostic Radiology

W. Reith

T. J. Vogl, W. Reith, E. J. Rummeny (Eds.), *Diagnostic and Interventional Radiology*,
DOI 10.1007/978-3-662-44037-7_3, © Springer-Verlag Berlin Heidelberg 2016

3.1 Technical and Physical Principles

A system for the diagnostic use of X-rays generally consists of an X-ray tube as the source of radiation, a high-voltage generator for operating the X-ray tube, an X-ray device with a recording system, and a fluoroscopic device.

The X-rays are produced by the deceleration of fast-moving electrons in the anode focal spot of the X-ray tube. For medical application, diagnostic and therapeutic X-ray tubes are used (Fig. 3.1).

The **X-ray tube** consists of:

- An electron source (cathode)
- A brake block (anode)
- A glass cylinder under high vacuum

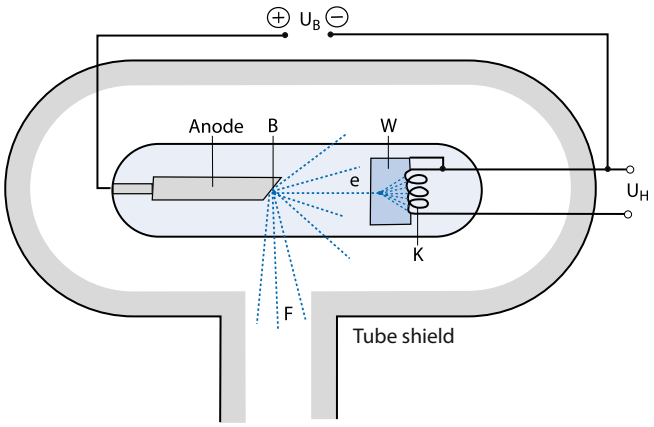

Fig. 3.1 X-ray tube, schematic illustration: anode; *B* focal spot; *R* tube shield; U_B acceleration voltage; U_H heating voltage; *F* beam exit window

The Cathode, Anode, and Glass Cylinder

In projection radiography (X-ray plain films, fluoroscopy images, contrast-enhanced radiographs for angiography, and venography) the X-ray beam is attenuated by absorption upon passing through the various tissues and used for imaging. The spatial distribution of the differentially attenuated X-rays is referred to as an X-ray intensity pattern. It is a summation of the absorption by the different tissues that occurred in the beam path (summation or projection image).

The ionising radiation is generated in X-ray tubes, which are surrounded by a protective housing. This protective housing has a double function. On the one hand, it limits the escape of the X-ray radiation to the beam exit window. On the other, it provides protection in the event of the X-ray tube exploding. Radiation is generated by heating a hot cathode. With temperature of the heating walls very high, the energy required for the electrons to exit the cathode material is applied. The cathode material is typically made of tungsten or a metal with a similar melting point. As a result of the voltage applied between the cathode and the pre-anode plate, thermally generated electrons are accelerated from the surface of the cathode to the anode. The impact is called the focal point or focus.

High-power tubes usually have two different-sized focal spots. The energy absorbed by an electron is determined by the X-ray tube voltage (U) applied. The fast incident electron is decelerated by the electric field of the atomic nucleus and deflected from its direction. The energy emitted is released as a quantum of X-ray bremsstrahlung. The efficiency with which this conversion takes place depends on the atomic number (Z) of the anode material, the voltage (U), and a constant.

Only 1% of the energy used is converted into radiation. The radiation thus generated is generally referred to as bremsstrahlung (braking radiation). The energy distribution of the quantum describes the X-ray spectrum. An increase in the X-ray tube voltage with equal mAs product, increases the dose rate. Additional filtering (e.g. with aluminium) serves to filter soft radiation components of the radiation that do not contribute to imaging (the majority are absorbed by the object) from the spectrum. In the radiator, the additional filtering of the radiation is equivalent to 2 mm of aluminium. This is also used in projection radiography for adults. In paediatric radiology, a higher aluminium equivalent is required, which is usually realised using an additional copper filter. Soft portions of the X-rays are more strongly filtered in the material than harder portions are; this effect is usually described as hardening of the radiation.

The proportion of the characteristic radiation at a molybdenum anode is significantly increased compared with radiation generated by tungsten. With an additional 30-µm molybdenum filter, the absorption edge of molybdenum almost completely cancels the K-line. This beam quality, which has strong proportions of characteristic radiation, is widely used in mammography. In mammography, rhodium is also used as an anode material along with molybdenum.

Scattered Radiation

Scattered radiation is generated when X-rays strike matter. All non-directional radiation in the useful beam is considered interference, just like the radiation that reaches the film or the digital detector surface outside the useful beam. This radiation does not contribute to imaging, but rather deteriorates image quality. Scattered radiation can be reduced by the following measures.

The most effective measure for the **reduction of scattered radiation** is the use of a grid (Fig. 3.2). These lead lamellae, which are parallel or orientated to the focus, are located between the patient and the film. The primary radiation is essentially radiated through the spaces between the lamellae. The scattered radiation that obliquely strikes the lamellae is absorbed. A small part of the primary radiation is also absorbed by the lead lamellae. Therefore, when using a grid, the radiation dose required to generate a sufficiently exposed X-ray image is slightly increased. During the exposure, the lead lamellae are removed so that they are not seen as lines on the radiographs. Grids are used when high-detail resolution is desired. In children younger than 7 years, no grid should be used to reduce the radiation dose.

Dose Rate

To estimate the individual dose rate for the exposure requirements of the patient, an automatic exposure control is used by default. Immediately in front of or behind the recording system in the beam path is a radiation detector that belongs to the automatic exposure and measures the dose rate. After reaching the pre-set dose rate, the radiation is automatically switched off.

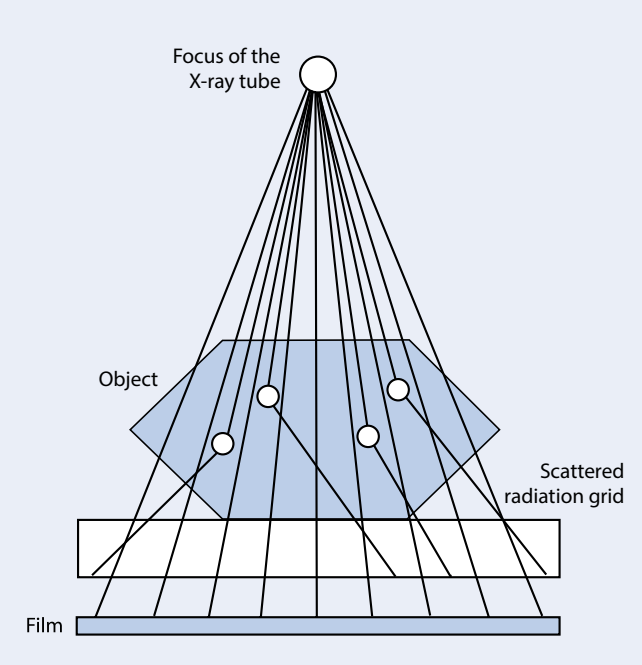

Fig. 3.2 Scattered radiation grid

3.2 Visual Documentation

X-ray Film

X-ray film has long been the medium of choice for recording and reproducing information. In the analogous projection radiography technique, the beam pattern emerging from the patient is reproduced as optical density on the radiographic film. Radiographic films are composed of a carrier layer, which is coated with photosensitive emulsion on both sides. The emulsion contains light-sensitive silver halide crystals (AgCr). These silver bromide crystals have a diameter of 0.7 nm and form development nuclei following exposure. During the film processing, the reduction process is amplified (development, unreduced silver salts are removed from the emulsion, fixing). The unexposed portions of the film become transparent, and the areas exposed by the X-rays are blackened. The film density is proportional to the intensity of the incident radiation. The intensity of the film density and the incident X-ray dose is not linear in all areas, but rather has an S-shaped curve. Even the smallest dose of X-ray radiation can blacken the film; each X-ray quantum absorbed causes a slight blackening of the film. On the other hand, only light rays of a certain intensity (threshold) can generate density. A certain number of quanta is necessary to achieve this effect.

In the under- and over-exposed image slices, there is no linear relationship between the dose and optical density. In the central part of the density curve that approaches linearity, there is a diagnostically useful exposure range of the corresponding film in which the attenuation differences in the radiation image can be converted into proportional differences in brightness in the film.

Intensifying Screens

In general, the X-ray film is located in the opaque film cassette between two intensifying screens, which reduce the dose required to generate optical density. The intensifying screens are stimulated to emit light by the incident X-ray. The intensifying screens therefore contribute to 95% of the film blackening; the X-ray radiation only contributes 5%. Compared with X-rays, the light quanta passing from the intensifying screens have an undirected course. Because of this, the film becomes blurred, although these effects are negligible in practice. Compared with screen-less films, modern films with rare earths as fluorescent substances have reduced the dose requirement by approximately 50%. The film systems are classified according to sensitivity. These differ in resolution capacity, in the noise component, and in the required dose. The guidelines of the German Medical Association for Quality Assurance in Diagnostic Radiology determine which sensitivity class should be used for a particular application area.

Quality

Image quality is determined by the sharpness and contrast. The contrast is influenced by the radiation characteristics, the radiation dose, the film characteristics, the reduction of scattered radiation, and the development process. Important factors that influence blurring include the motion of the object, the film and tube, the film–foil combination, the size of the focal spot, and distance geometry. The X-ray itself causes a certain fuzziness, which is subject to the following laws:

- The larger the focal spot, the greater the blurring.
- The greater the distance between the focal spot and the object, the lower the blurring.

At a constant image focal distance, the magnification effect can be calculated if the object on the area close to the film is brought to the area of the beam path near the X-ray. Object areas close to the tube are thereby magnified and more blurred compared with objects close to the film. With increasing distance from the vertical projection, geometric structures are distorted in the periphery of the image.

Image Development

Images are currently developed in automatic developing machines, in which the exposed film is automatically removed from the cassette and the cassette is reloaded with unexposed film from a connected supply magazine.

3.3 Testing Equipment/Procedures

3.3.1 Contrast Agent-Assisted Recordings

The most common fluoroscopically targeted images are **contrast-enhanced images** of the gastrointestinal tract, fistula and vascular imaging. During fluoroscopy, mobile X-ray and tiltable mounting tables for specific settings are implemented according to the anatomical conditions. With a low-angle view, dynamic studies can be performed. This examination technique is required for the following tests:

- Gastrointestinal tract (examinations of the oesophagus, stomach, small intestine, and colon)
- Vessels (arteriography and venography)

- Depiction of the passageways of exocrine glands (endoscopic retrograde cholangiopancreatography, cholecystangiography, sialography, galactography, and dacryocystography)
- Joints (arthrography)
- Spinal subarachnoid space (myelography)
- Efferent urinary tract (retrograde ureteropyelography, urethrography, voiding cystourethrogram)
- Depiction of fistula

Modern screening devices employ **pulsed X-rays** to reduce exposure to radiation. The pulse sequence can be chosen based on the temporal resolution required at various stages.

In fluoroscopy, the dose rate is higher than for X-ray imaging performed with grids.

To reduce exposure to radiation and to improve the signal-to-noise ratio, **image intensifier television chains** are used in fluoroscopy. The image intensifier consists of a vacuum vessel, an input screen in front and an output screen behind. The input screen is found on the interior of the vacuum vessel. It is composed of the fluorescent layer (caesium iodide) and the photocathode. The caesium iodide absorbs a large part of the incident X-ray photons.

At sites struck by light quanta, the photocathode releases electrons via the photoelectric effect. The free electrons are accelerated in the high-voltage electric field between the photocathode and the output screen. The electron image in the vacuum tube corresponding to the X-ray intensity pattern behind the patient is converted into a photograph via fluorescent effects in the phosphor layer of the output screen. Compared with the input image, it is reversed and more intense.

Fluoroscopically targeted images can be mapped onto analogue film or digital imaging plates (**direct recording technique**).

In the **indirect exposure technique** the amplified output image is directed either onto a 100-mm camera (medium format technology) or a cine camera.

In digital image intensifier radiography, the analogue signal of the video camera is converted into a digital signal. After processing in the image computer, the digital image data set is transmitted to a laser camera where it is documented on film or stored on optical media.

Digital Subtraction Angiography

Digital subtraction angiography (DSA) is a temporary filtering technique that allows the isolated representation of vascular contrasts after the administration of contrast agent (Fig. 3.3). It is a special form of digital image intensifier radiography. In general, image data sets are prepared before and after the administration of intravascular contrast agents. The image data sets are then subtracted with and without vascular contrasts so that the static image elements of the vascular environment are mathematically eliminated and only vessels perfused with contrast agent are displayed.

By eliminating the background, the skeletal and soft-tissue structures disappear. Incongruent subtraction occurs if there is an incongruence of mask and filling image resulting from patient movement during the DSA series. There are various options available for the **correction of this incongruity**

- **Pixel shifting:** "pixel shifting" is performed to eliminate incongruence.
- **Re-masking:** by selecting a different, non-default mask image, incongruities can be reduced or eliminated.
- **Image integration methods:** image integration significantly improves the signal-to-noise ratio. For example, the first image can be integrated and subtracted from the vascular filling images.
- **Vascular tracing:** upon injection of a small bolus of contrast agent, a longer vascular route can be represented by summing several DSA images. During a series, the small bolus of contrast agent migrates along a vascular route. On the initial images it can be seen in the central arteries. It can later be seen in the peripheral arteries. The combination of the selected images gives a continuous representation of the vascular tree to be examined. The method also reduces the signal-to-noise ratio.
- **Road mapping/pathfinder technology:** road mapping helps the examiner to position the catheter in the vessel. Under fluoroscopy, a small amount of contrast agent is injected into the catheter. As soon as the vessel contrasts, the examiner interrupts the fluoroscopy, and the computer stores the last image as a mask. After restoring the fluoroscopy, subsequent fluoroscopic images are continuously subtracted from the mask. The investigator can directly locate the vessel and the position of the catheter.

Myelography

Fundamentals and Preparation of the Investigation

In myelography, the CSF-filled cavity surrounding the bone marrow is filled with contrast agent. The spinal subarachnoid space communicates with the skull and the cerebral ventricles. Water soluble contrast agents are used. Before the examination, the patient must be informed of possible complications such as an allergy to the contrast agent, bacterial or non-bacterial meningitis, arachnoiditis, cranial nerve deficits, paraplegia, and intra-spinal haemorrhaging.

Briefing the Patient. Myelography can be seen as an invasive examination technique, which is burdensome to the patient. The patient must be legally informed about the course and objective of the examination at least 24 h in advance. The patient must also be informed about the side-effects that may result from the puncture and the injection of contrast agent. These include nausea, vomiting, and headache and may persist over several days. The patient must even be informed about rare complications such as haemorrhaging in the spinal canal (possibly with a subsequent indication for surgery), paralysis, hearing and vision problems (especially paralysis of the abducens nerve), infections with epidural or intadural abscess and meningitis, and the possible aggravation of pre-existing symptoms.

Contra-indications. It must be ensured that the patient does not suffer from any coagulation disorders. Acetylsalicylic acid (aspirin), which is often used as a pain reliever and anti-coagulant,

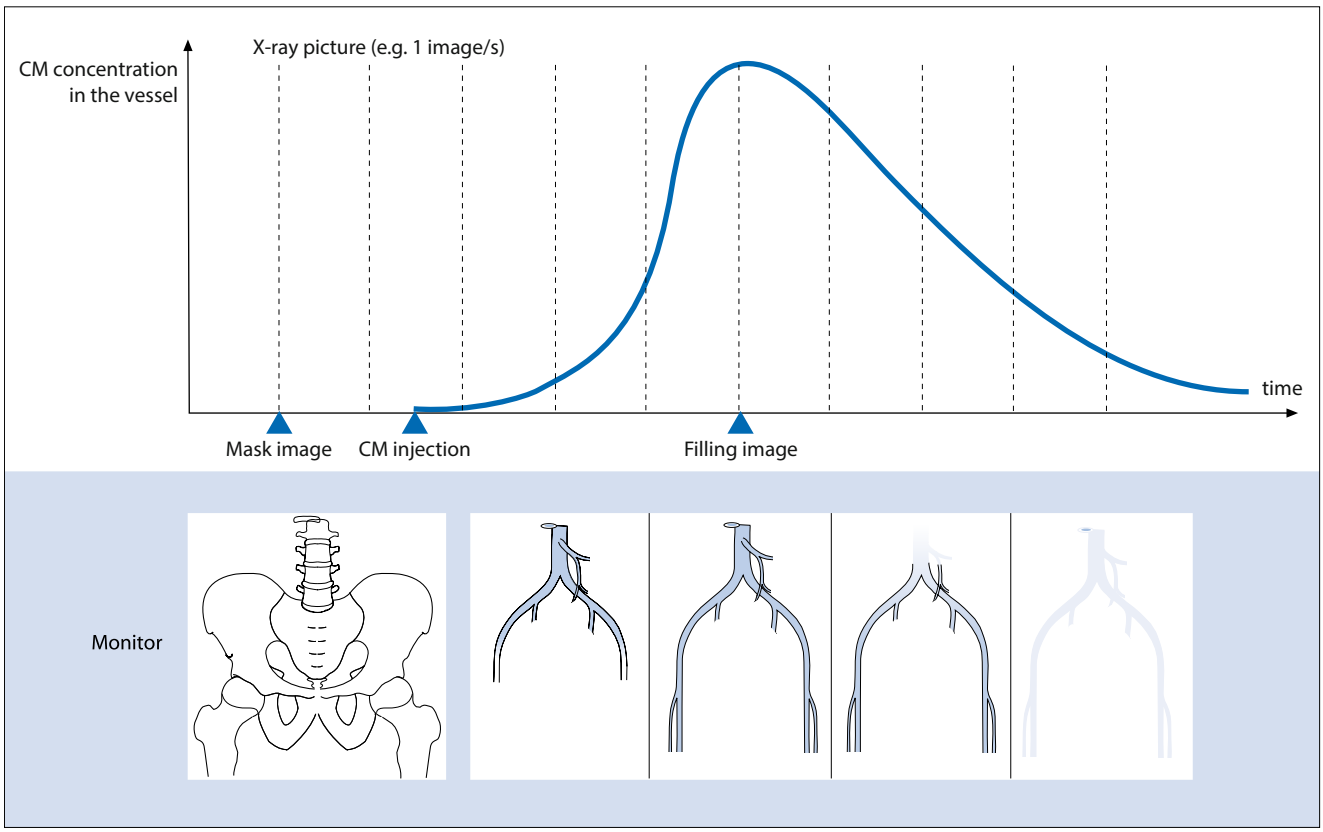

Fig. 3.3 Function principle of digital subtraction angiography

should be continued 3–4 days before the examination – even in low doses. The thyroid values should be available. In the case of overt hyperthyroidism, these should be clarified beforehand. Another investigation modality may be applied.

An increase in intracranial pressure is an absolute contraindication for myelography. In the case of severe dysfunction of the liver, kidneys, and lungs as well as heart and circulatory weakness, a strict benefit–risk assessment is required. In principle, a spinal CT and/or MRI investigation should have been performed.

Procedure after Investigation. After the examination, the patient should drink at least 3 l of fluids (e.g. water or tea) over a 24 h period. The previously prescribed 24-h bed rest is not necessary because no clear causal relationship has been found between headaches and bed rest.

Conducting the Examination

As a rule, a non-ionic contrast agent is injected into the subarachnoid space (see below); a puncture at C1/C2 is now rarely performed. Before injection, CSF is taken for diagnostic and chemical analysis.

Myelography can be performed on the seated or supine patient on a fluoroscopy unit with a swivel seat. The puncture of the CSF is done with a special needle (Yale Spinal 22 G) and involves minimal pain and risk. The typical puncture height is C4/C5, but C4/C5 or C2/C3 can also be used because the cone is usually found at the height of T12/C1. (Fig. 4.3). At the beginning of the contrast agent application, a short fluoroscopy is required in order to ensure a safe intrathecal location.

After puncture and Trendelenburg positioning of the patient, the contrast agent is allowed to flow in the cranial direction under continuous fluoroscopic guidance. It will be clear whether the spinal canal is continuous. For lumbar myelography, 10 ml of an anionic, iodinated contrast agent (e.g. Isovist or Solutrast) with a concentration of 240 mg iodine/ml is injected. For a cervical myelography and pan-myelography, up to 18 ml of contrast agent with a concentration of 30 mg iodine/ml is injected.

It is important to ensure that the contrast agent does not pass intracranially through the foramen magnum. This could otherwise increase the likelihood of neurotoxicity-induced generalised seizures. Therefore, from some investigators, 10 mg diazepam is applied intravenously before cervical myelography and pan-myelography to minimise this risk. The benefit of this has yet to be established.

For lumbar myelography, after documenting the needle position one antero-posterior, one lateral, and one or two oblique images are acquired. Finally, the functional images and images of the cone area are connected.

Lumbar myelography:

- Lateral imaging with documentation of the location of the puncture needle
- Antero-posterior imaging

- Oblique image, approximately 45% under free rotation of the root in both directions
- Imaging in ante- and retroflexion
- For CT myelography, the patient must be positioned in the prone position with a lowered head.

For **cervical myelography**, the following images are recommended:

- Postero-anterior inclusion in hyperextension of the head showing the cranio-cervical junction and the cisterna magna.
- Postero-anterior view of the middle cervical spine segments and the cervico-thoracic transition region in the case of congruent chin and occipital scalp.
- Two images in 15–20° right and left anterior oblique projection.
- Images with the cassette in the prone position with a laterally retracted second tube and a complete representation of the seventh cervical vertebra and the cervico-thoracic transition region.
- Lateral imaging with the patient standing with an extended cervical spine.
- Lateral recording with the patient standing with an anteflexed cervical spine.

CT Myelography

Following intrathecal administration of a water-soluble, iodine-containing contrast agent (e.g. Isovist) spinal CT proceeds via a lumbar puncture in the framework of myelography followed by post-myelo-CT after an appropriate temporal interval of 20 min to 4 h (Fig. 3.4). CT myelography should be performed either via an incision parallel to the intervertebral discs or in spiral mode.

As a rule, intrathecal administration of contrast agent results in a good delineation of the spinal cord and the nerve roots within the root pouches. The number of segments to be tested depends on the myelographic findings and the clinical symptomatology. To detect additional degenerative spine changes, the complementary documentation of HR bones is essential.

When diagnosing intervertebral disc disease, 2- to 3-mm slices should be made parallel to the intervertebral disc space. This should include areas from the vertebral arch of the disc located above the intervertebral disc compartment to the vertebral arch of the disc located below the intervertebral disc compartment. The gantry tilt, i.e. the angulation of the layer plane relative to the longitudinal body axis, is thereby re-adjusted for each level. CT scans are performed in the soft tissue and bone windows.

After injecting the contrast agent, target images are taken in the appropriate slices. The inclination of the tilting table and the rotation of the patient should allow a relatively superposition-free representation of anatomical structures and pathological changes. In addition to the images in the neutral position, images in functional positions (retroflexion, anteflexion, and functional myelography) can be documented.

In addition to the indirect myelographic representations, after completion of the myelogram, a post-myelographic CT scan, which utilises the high contrast between the CSF and surrounding soft tissue structures, is performed.

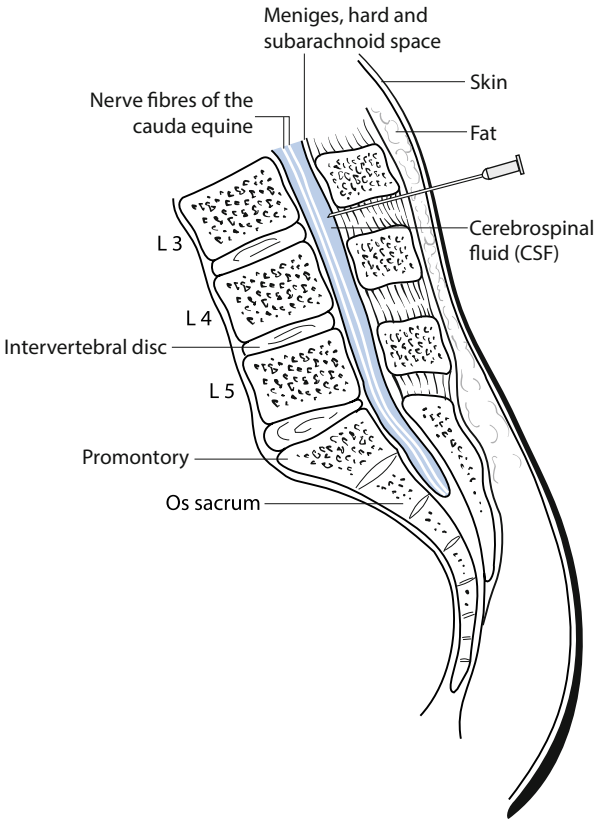

Fig. 3.4 Schematic representation of the puncture site for lumbar puncture, e.g. for myelography

Computed Tomography

W. Reith

T. J. Vogl, W. Reith, E. J. Rummeny (Eds.), *Diagnostic and Interventional Radiology*,
DOI 10.1007/978-3-662-44037-7_4, © Springer-Verlag Berlin Heidelberg 2016

4.1 General

Computed tomography is one of the most important techniques of radiological diagnosis. The first computed tomography technique was developed by Godfrey Hounsfield and was first used for skull examinations in 1971. In 1974, the first whole-body computed tomography technology was installed.

Computed tomography is based on a tomographic X-ray technique in which an X-ray beam scans the patient from different directions. Through parallel collimation the X-ray beam is formed into a thin fan, which defines the layer thickness. As it passes through the body, the X-ray is attenuated and detected. Using mathematical image reconstruction, the local X-ray attenuation is then reconstructed into so-called CT values and greyscales, coded, and finally displayed as an image.

In first- and second-generation CT devices, the X-ray tube only moved in two single movements: translation and rotation. In third- and fourth-generation devices, the X-ray tube rotates around the patient. With a collimator system, a narrow fan and thus the X-ray is masked out from the radiation cone. Its width corresponds to the desired thickness of the body slice. Because the scanners of the third generation have better scattered radiation suppression and fewer detector elements, this technology is used in all current multi-detector systems.

Electron Beam CT. Here, an electron beam with a voltage of 120 kV is accelerated into a funnel-like vacuum tunnel and deflected onto targets by deflection coils, which are placed under the patient in a semi-circular pattern. The individual targets correspond to the anode of the X-ray tube; the X-radiation is formed on them. The electron beam is attenuated via a semi-circular detector situated around the patient.
One advantage of electron beam CT is the extremely short scan times for individual layer thicknesses; practically no motion artefacts occur. However, disadvantages are the poor image quality caused by noise. Multiple measurements for improving image quality require longer scan times and higher doses.

4.2 Key Technical Characteristics of Computed Tomography

Image Reconstruction

The CT scan measurements and data are pre-processed in order to correct for variations in the detector system and beam hardening artefacts of the X-rays. Upon passing through the patient, the attenuation of the X-rays is determined in each position of the X-ray tube, logarithmised, and back-projected following high- and low-pass filtering (convolution kernels) using a line integral (convoluted back projection). By superimposing the attenuation values of all projections, a photograph is produced; each two-dimensional image (pixel) represents a volume element (voxel).

The image reconstruction begins with the definition of the field of view (FOV) of interest. A CT image consists of a square image matrix, which is typically 1,024 × 1,024 pixels in newer devices. Each CT slice has a defined thickness, and each pixel corresponds to a volume element (voxel). The size of the voxel is obtained from the matrix size, the selected field of view, and the layer thickness. In most studies, the voxels are bar-shaped, i.e. the XY plane is generally smaller than the slice thickness (Z-direction). This anisotropy of the voxels can usually only be reduced by reducing the slice thickness. With a modern multi-detector CT system, a nearly isotropic voxel is achieved.

Table 4.1 Typical CT density values in Hounsfield units

Tissue	Hounsfield units
Lungs	−500
Fat	−100 to 0
Water	0
Liver (native)	40–60
Fresh blood	70–90
Liver after the administration of contrast agent	Approximately 150
Cancellous bone	Up to approximately 300
Compact bone	300–1,000

In the image reconstruction, each voxel is assigned a numerical value (CT value), which is a measure of the X-ray attenuation (μ) in that voxel. The CT values are given in Hounsfield units (HU) (Table 4.1). The Hounsfield scale starts at −1,000 for air, has a value of 0 for water, and has no upper limit, although this is usually given as 3,000 (Fig. 4.1). The available CT value range is device-specific and varies depending on the bit depth (bits per pixel) (e.g. from −1,024 to 3,071 HU for 12 bits or up to 64,500 HU for 16 bits).

The definition of the CT value is as follows:

$$CT = 1{,}000 \times \frac{\mu - \mu H_2O}{\mu H_2O} (HU)$$

Because the human eye can only distinguish between approximately 40–100 shades of grey, the entire range of the grey scale is represented on the CT scale. Only a portion of the CT scale, the so-called window, is depicted. The window is defined by its width and location (also called level or centre). The width determines the image contrast, the brightness level. A narrower window leads to contrast enhancement and improved representation of low-contrast structures. A wide window leads to contrast reduction and improved representation of structures with greatly differing CT values, e.g. bone and pulmonary parenchyma. Through the choice of the window, the density values above and below this window are uniformly black or white. Tissue or pathological changes in which the density roughly coincides with a reference value (e.g. water, brain) are isodense. Changes in which the density is higher than the reference density values are hyperdense, while changes in which the density is lower than the reference density values are hypodense.

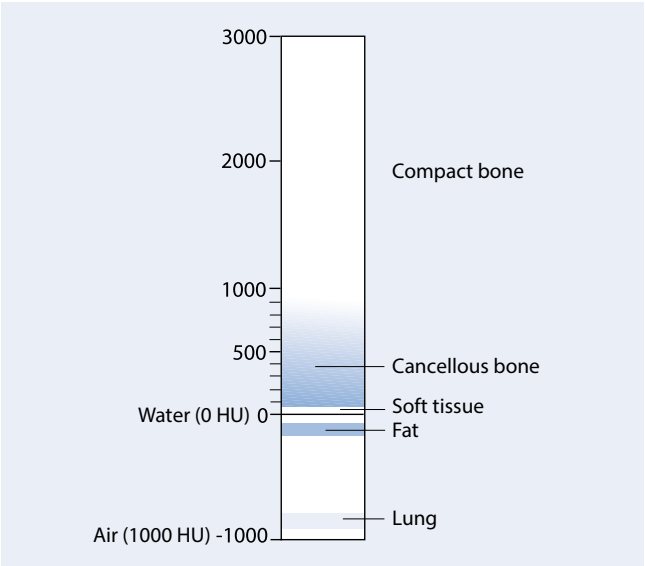

Fig. 4.1 Scale of CT values. The scale is defined by a value of 0 HU for water and −1,000 HU for air; soft tissue has values of around 50 HU

Gantry Tilting

Depending on the manufacturer, the scanner unit (gantry) can be tilted up to ± 30° about the X-axis in order to obtain oblique slices. However, in modern multi-detector scanners, it is often not necessary to tilt the gantry.

Slice Thickness

The collimation of the X-ray tube determines the thickness of the slice under investigation. As with conventional X-ray diagnostics, the X-ray tube emits conically diverging radiation. The X-ray beam must be masked out via the collimator (collimation). However, an exact plane-parallel slice can never be achieved. In addition to the primary beam, the X-ray tube produces a half shadow, the so-called penumbra (Fig. 4.2). Because of the beam geometry, regions outside of the selected layer are also detected. This results in a rounded off slice sensitivity profile, which roughly corresponds to an ideal rectangular profile for the collimation of large slices. The full width at half maximum (FWHM) of the slice profile is used as a measure for the effective thickness. The effective thickness is a measure of the resolution along the patient axis (Z direction).

In modern spiral and multi-detector CT scanners, the effective layer thickness and the slice collimation are not necessarily consistent.

Partial Volume Effect

Because of the rectangular geometry of the voxels, it is often the case that not only objects of interest (e.g. a nodule) contribute to the CT value in the voxel, but also the surroundings according to their volume fraction. The resultant CT value of the voxel is thus slightly distorted and represents the sum of the various attenuation values (partial volume effect) (Fig. 4.3).

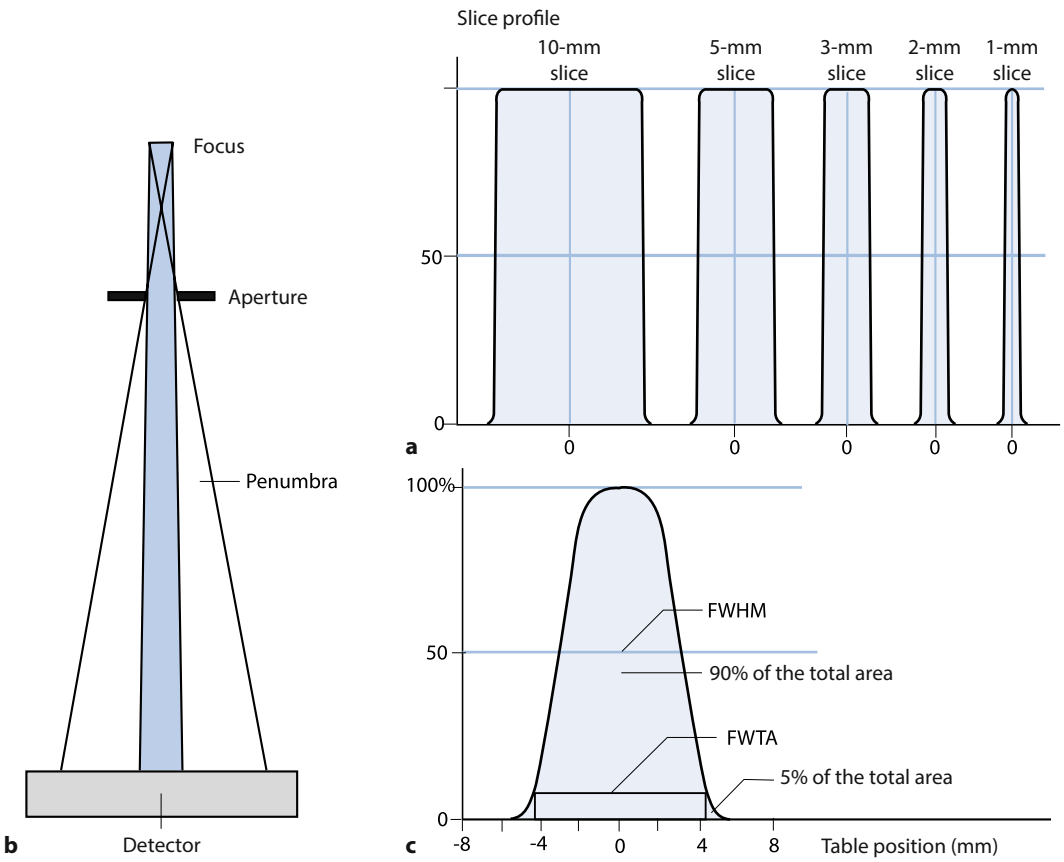

Fig. 4.2a–c Schematic representation of the slice thickness. **a** Because of the beam geometry, regions outside the selected layer thickness are also recorded. **b** The resulting "slice sensitivity profile" only approaches an ideal square for large slice collimations. **c** FWHM as a measure for the effective slice thickness

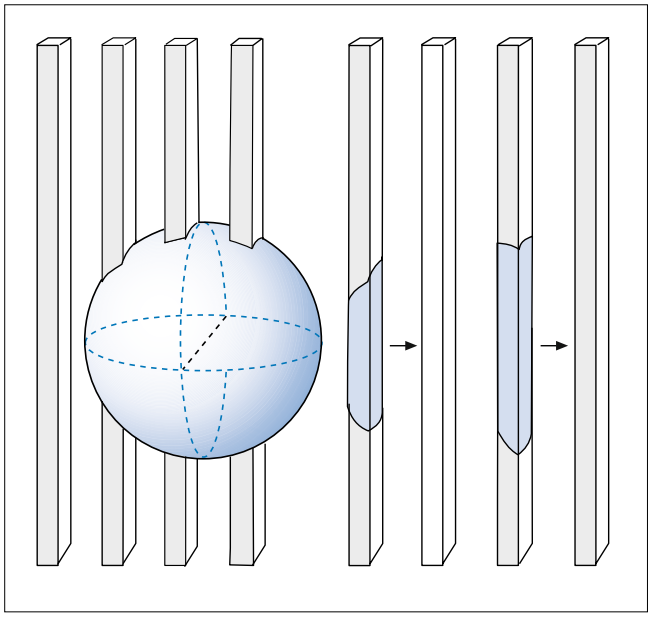

Fig. 4.3 Partial volume effect. The voxels are like a matchstick or rectangle; in addition to the objects of interest, the environment (according to the volume fraction) contributes to the CT value in the voxel. This leads to a distortion of the CT value of the voxel

Slice Collimation

Because of the axial slicing typical for CT, structures extending vertically and parallel along the body axis only display low partial volume effects. Partial volume effects are problematic for small structures or those that are diagonal to the scanning axis (e.g. the diaphragm and renal pole). For structures extending parallel to the plane of the slice (e.g. the pancreas and adrenal glands), collimation should be reduced to 3 mm. Thin collimation of 1–2 mm slice thickness is used in the diagnosis of interstitial lung disease, which requires visualisation of the finest structures.

4.3 Multi-Detector CT

Unlike systems with a single detector ring (one-slice CT), multi-detector systems have two or more parallel detector rows, which can simultaneously record raw data. The first systems with four parallel active detector rows were introduced in 1998. There are now devices with 6, 8, 10, 16, 20, 32, 40, 64, 128, and 256 rows. The performance of these systems is further enhanced by a higher rotational speed. The rotation time is 0.3 s, which is particularly advantageous in cardiac diagnostics. The spiral data acquisition is often used, especially for large volumes of investigation in the abdomen. A sequential mode (layer by layer) is also possible; this is often used to examine the lungs (HR-CT) and neurocranium or in interventions.

The advantages of multi-detector CT are the shorter sampling period with reduced motion artefacts, especially in children, accident victims, and critically ill patients. The longer examination sections are advantageous for depicting vessels. The thinner collimation and thus thinner layers result in virtually isotropic imaging. This is particularly advantageous in depicting the temporal bone and musculoskeletal system with multi-planar reconstructions.

4.3.1 Acquisition Parameters

As with conventional spiral CT, for multi-detector CT, the most important acquisition parameters are slice collimation, table feed per rotation, and pitch. In addition to the reconstruction increment, the effective slice thickness or slice width is another important reconstruction parameter.

It is important to distinguish between acquisition and reconstruction parameters.

Slice Collimation

The slice collimation available on a multi-detector CT is determined by configuration of the detector. Slice collimation determines the spatial resolution in the Z direction. For high-resolution filters such as those used for skeletal and lung diagnostics, collimations < 1 mm are required. The smallest reconstructable slice width is identical to the collimation. The possibility of reconstructing isotropic data is lost with the use of thicker slice collimation.

Rotational Speed

The rotational speed describes the duration of a full rotation of the X-ray tube around the patient. The newest scanners have rotational speeds to the order of 0.33–0.42 s. To get even more effective spin times, a scanner with multiple X-ray tubes (dual-source technology) is a suitable alternative. For limited mechanical tube load, higher effective rotation times can be achieved, which is particularly well suited to cardiac imaging.

Two-Tube Technology (Dual Source)

In dual-source technology, two X-ray tubes and two detector rings are used to improve the temporal resolution. This technology was developed for cardiac CT. By using the two acquisition systems, the image acquisition time can be halved. Another potential advantage is the use of two tubes of different voltages (kV). The difference in X-ray absorption at identical projection angles can be used to separately represent materials with different atomic numbers (e.g. calcium, iodine, and soft tissue).

Pitch

In multi-detector systems, the pitch is defined by the ratio of table feed per rotation for total collimation:

$$P = \frac{TF}{N \times SC}$$

The pitch can vary between 0 and 2 without the occurrence of sampling gaps (Fig. 4.4). A low pitch factor leads to fewer cone beam artefacts, but requires a higher radiation dose for the same noise ratio. If a thin-slice collimation and a higher pitch factor are used, high-quality multi-planar reconstructions can be obtained from the raw data. With 16- and 64-row scanners, these differences are less relevant because thin slices are used anyway.

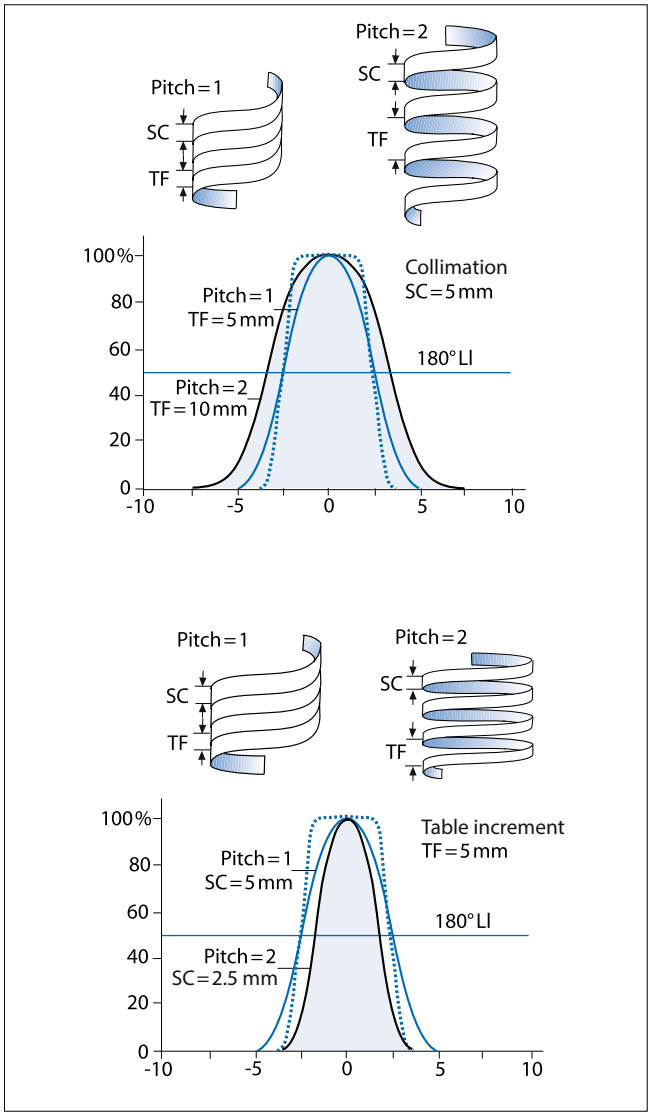

Fig. 4.4a–d Pitch factor. **a** An increased pitch factor leads to "pulling apart" of the spiral. **b** At constant collimation, the slice profile is expanded. A pitch of 2 and the slice profile at 180° linear interpolation (LI) corresponds to a pitch of one and the slice profile of 360° LI (see also **c**). When the pitch increases from 1 to 2, the slice profile only increases by 30%. However, the increase in pitch doubles the scan length. **c** If the pitch is increased, the collimation (SC) simultaneously decreases. The scan length remains unchanged. **d** However, this results in a slice profile that is 35% narrower at 180° LI

Scan Time

The scan time is calculated from scan length and table speed. The table speed is calculated from the table feed per rotation and the rotation time. The scanning time increases proportionally to the rotational time and inversely proportionally to the detector width and the pitch.

4.3.2 Reconstruction Parameters

Slice Width

The slice width may be less than or just equal to the collimation. The slice width depends on the manufacturer and is determined by Z-filtering and the cone-beam algorithm. A slice thickness that is identical to the collimating always has a higher noise and should therefore only be used for studies in which the highest possible resolution in the Z-axis is required.

Reconstruction Increment

The reconstruction increment can be set in a similar manner to conventional spiral CT. For normal reporting, a moderate overlap of approximately 20% of the film thickness is sufficient. An optimal quality of MPR or 3-D data sets requires an overlap of about 50%; the voxels are thus roughly isotropic. In most body examinations, the pixel size in a field of view of 30–40 cm is between 0.6 and 0.8 mm. A reconstruction increment of exactly the same size thus produces an isotropic grid of pixels.

4.3.3 ECG Synchronisation in Cardiac CT

For cardiac imaging, but also for the analysis of pulsation effects, ECG synchronisation of the data acquisition is necessary. Two techniques are available: prospective ECG triggering and retrospective ECG gating. In prospective ECG gating, the data are sampled within a predefined interval of the RR cycle. In retrospective ECG gating, the data are acquired during the entire cardiac cycle and retrospectively reconstructed in different phases. In order to eliminate cardiac motion and minimise artefacts, a high temporal resolution is necessary. For a sharp imaging of the heart without motion artefacts, temporal resolutions of 50–100 ms in end-systole and 100–200 ms in mid-diastole are required.

4.4 Imaging and Presentation Techniques

Cine Mode

Cine mode is an excellent tool for analysing large numbers of cross-sectional images. A large number of slice images can therefore be seen quickly. It is important that the image sequence and speed can be controlled.

Multi-Planar Reconstruction

In multi-planar reformation, two-dimensional raw images from axial image data are reconstructed in arbitrary planes (Fig. 4.5). Coronal or sagittal reconstructions are created by selecting and displaying each overlying voxel in the corresponding plane. Curved reconstructions (curved planar reformation) are used to display structures that cross multiple axial slices of a volume. The quality of MPR images will improve if the slice plane differs slightly from the scan plane. The resolution in the Z-axis should be minimised in order to improve the image quality. Sequential examination techniques and wide collimations lead to level artefacts in reconstructions perpendicular to the plane of examination. A thin collimation and thin layer width allows reconstructions of outstanding quality in any cutting direction.

For larger pitch factors, level artefacts or serrations occur in structures located outside of the gantry centre or diagonally through the slice layer. These artefacts result from the interpolation of a scan of the data in the Z direction (under sampling).

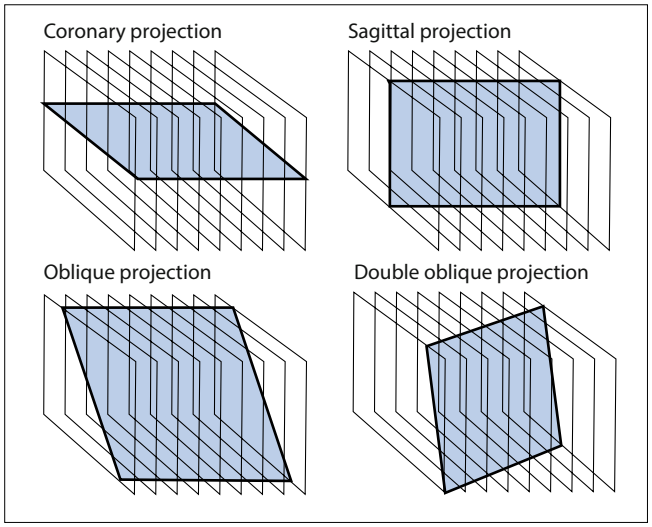

Fig. 4.5 Reconstructed multi-planar tomograms. Various projections, shown schematically

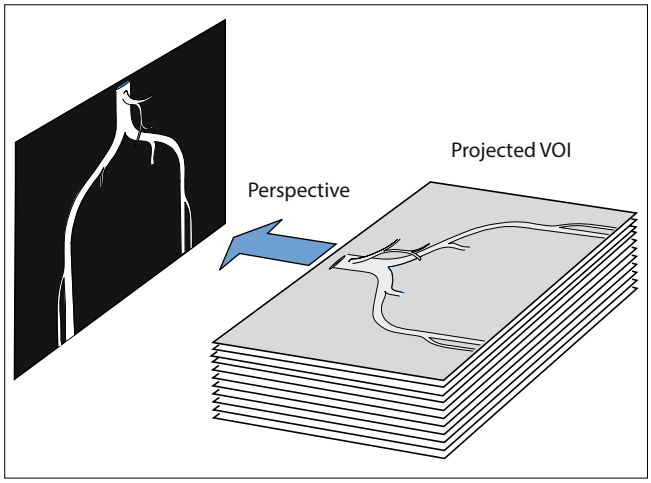

Fig. 4.6 Principle of maximum intensity projection (MIP). With this technique, the maximum CT values are projected perpendicularly to the viewing plane. Through additional editing of the data volume, bony structures are eliminated so that the vessels can be represented

Maximum and Minimum Intensity Projection

Maximum and minimum intensity projections (MIP and MINIP) are volume rendering procedures. First, the volume to be displayed is determined by using the appropriate editing procedure. MIP techniques are used in CT angiography and in special pulmonary issues (Fig. 4.6). MINIP mainly serves to present the tracheobronchial system. The actual images are generated by projecting the volume of interest onto the viewing plane. An MIP represents the maximum CT value along the projection volume, while an MINIP represents the minimum value. For MIP representation, optimal image quality requires the narrowest possible presentation volume (VOI).

The advantages of the MIP images are that contrasted vessels and wall calcification can be differentiated because of differing CT values. Smaller vessels with a 1-mm diameter also remain visible as long as they have a higher CT value than their surroundings within the VOI. An optimal image contrast is achieved at high intravascular contrast, low partial volume, and low background density.

In the case of an overly large VOI and relatively dense surrounding structures, smaller vessels with lower or identical density are no longer visible relative to their surroundings. Intravascular lesions such as mural thrombi or soft plaques are often not directly displayed by MIP. Dissection membranes are also often not represented. Calcifications have a higher density and thus project themselves via the vascular structures. It is often not possible to properly evaluate the degree of stenosis.

For MIP, the major field of application is CT angiography. However, it is not recommended for the diagnosis of complex vascular malformations, aortic dissection, pulmonary embolism, or central-floating thrombi.

3-D Surface Reconstruction (Shaded Surface Display)

3-D surface reconstruction is a method by which three-dimensional images can be reconstructed from surface structures. The object is illuminated by a virtual light source, and the software calculates the reflection of the light intensity back to the viewer

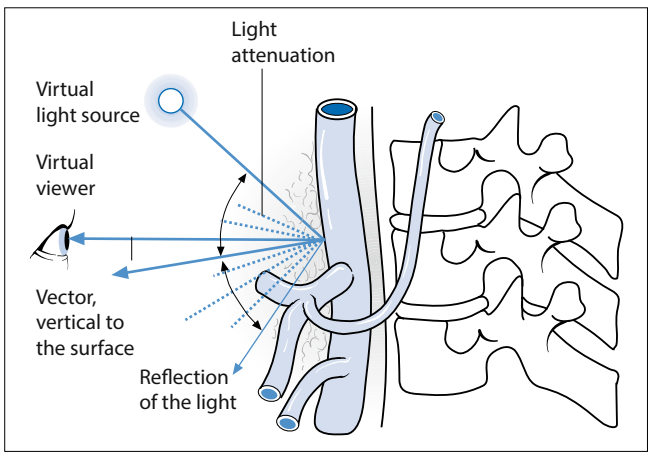

Fig. 4.7 Surface reconstruction. Special software calculates the reflection of the light from a virtual light source from the displayed object back to the viewer, thereby making surfaces appear three-dimensional

(Fig. 4.7). However, the VOI must be clinically defined and sequenced. 3-D surface representation provides impressive images of defined surface structures in complex topographies. 3-D surface representation is primarily used to present findings. For the diagnostic process, it is only suitable in exceptional cases. It is used mainly in skeletal diagnostics. As a result of virtual endoscopy, 3-D surface representation has become more important because compared with the volume reconstruction technique, the process is much faster. It is suitable for interactive navigation through virtual endoscopic datasets.

It should be noted, however, that the selected threshold range can seriously affect the quality of the 3-D surface representation.

Magnetic Resonance Imaging

W. Reith

T. J. Vogl, W. Reith, E. J. Rummeny (Eds.), *Diagnostic and Interventional Radiology*,
DOI 10.1007/978-3-662-44037-7_5, © Springer-Verlag Berlin Heidelberg 2016

5.1 General

The basis for an understanding of the theory and practice of MRI is a basic knowledge of magnetism and electricity. Magnetism is based on electricity. Since the first half of the 19th century, it has been known that electric currents create magnetic fields. Physicists measure magnetic field strength in amperes per meter (A/m). Magnetic field density is measured either in Gauss (G) or in the modern SI unit Tesla (T). One Tesla corresponds to 10,000 Gauss. The unit Tesla is often used to indicate the magnetic field strength. Most clinical MR devices operate in the range 0.5 to 1.5 Tesla. MRI uses both static and variable magnetic fields. Furthermore, it requires high-frequency waves (HF). Magnetic resonance signals are time-dependent electric currents or voltages. They are formed in waves, which are induced by an oscillating magnetic field. Magnetic resonance signals are essentially sinus and cosine waves, which are defined and described by three factors: amplitude, frequency, and phase.

The **amplitude** is also referred to as signal strength and corresponds to the final brightness of the image elements of a magnetic recording.

Frequency and phase determine the form and spatial resolution of the MR image. The phase determines the output amplitude of a wave and can only be compared for waves of the same frequency. Phase differences are given in degrees. If two waves of the same frequency are shifted against each other, this results in a phase shift. Signals are transmitted by changing electromagnetic radiation. In MRI, this is divided up into pulses, which can be sent in different orders.

The bandwidth includes the frequency range of the pulse. In analogue systems, bandwidth is defined as the difference between the highest and lowest frequency component of the signal. Radiofrequency pulses have a certain waveform and change in the time domain. Using pre-transformation, the pulses can be better analysed.

The principles of MRI were discovered by the groups of Russell and Bloch. In 1952, both researchers were awarded the Nobel Prize for Physics. In 1973, Lauterpur published the first MRI image. However, the importance of MRI as a digital medical imaging procedure was only first realised in the early 1980s.

5.2 Physical Principles of MRI and Characteristics of Image Formation

Nuclei containing an odd number of protons or neutrons have an intrinsic angular momentum or magnetic resonance in the basic state.

Relaxation

After the spins are excited, the magnetisation gyrates in the XY plane. This so-called transverse magnetisation (M_{xy}) generates the MR signal in the receiving coil. Two independent processes ensure that the transverse magnetisation and thus the MR signal decrease and that the stable initial state is achieved before the excitation. On the one hand, these are the so-called spin–lattice interactions and on the other, spin–spin interactions. The two processes are referred to as T1 and T2 relaxation.

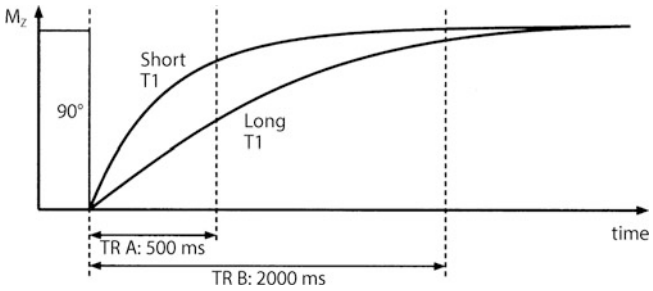

Fig. 5.1 Repetition time (TR) and the T1 contrast. With short TR (*A*), a tissue with a short T1 again displays a great deal of longitudinal magnetisation and generates much signal. Tissue with a long T1, however, produces little signal. For long TR (*B*), both tissues have accumulated similarly large magnetisation and generate approximately the same amount of signal. (From: Weishaupt et al. 2006)

T1 Relaxation

With time, transverse magnetisation returns to the Z direction. The transverse magnetisation remaining in the XY plane also slowly decreases; the MR signal becomes correspondingly smaller. For this, the longitudinal magnetisation (M_z) slowly rebuilds – longitudinal relaxation. With the release of energy, it is connected to the surroundings. The time constant of this process (T1) depends on the strength of the external magnetic field (BO) as well as the inner movement of the molecules. For tissues, this is to the order of one half to several seconds (Fig. 5.1.).

T2/T2*: Transverse Relaxation

Transverse relaxation is the loss of the transverse magnetisation through the de-phasing of the spins. No energy is dissipated to the surroundings, but rather the spins exchange energy with each other. Transverse relaxation has two components:

The spins exchange energy with each other via fluctuating, sometimes rapidly changing local magnetic field changes, which are caused by adjacent spins. The pure spin–spin interaction is not influenced by a 180° pulse. The time constant is T2 and is more or less independent of the strength of the magnetic field (BO).

Temporal constants, i.e. always equally strong heterogeneity of the external magnetic field (BO) are caused by the MR device itself as well as the body of the person under examination. They produce an additional magnetic field change so that the signal does not decay with T2, but rather rapidly with a time constant T2*. The relaxation time T2* is generally shorter than that of the T2 time. The majority of the heterogeneities that make up the T2* effect appear at tissue interfaces or are induced by local magnetic fields, e.g. iron particles. The T2*-decaying MR signal is also referred to as free induction decay (FID). The T2* effect can be eliminated by means of spin-echo sequences.

T2 describes the actual process of exchanging energy among the spins (Fig. 5.2). Additional heterogeneities lead to additional phase decay, which is characterised by T2*.

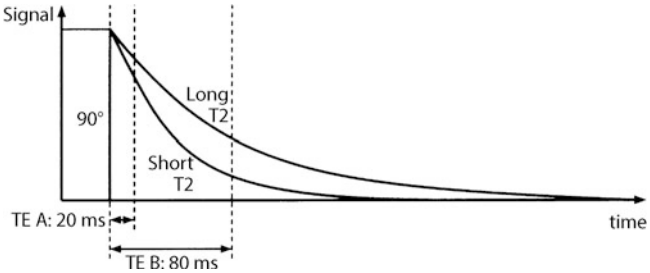

Fig. 5.2 Echo time (TE) and T2 contrast. For very short TE (*A*), there is still virtually no signal drop in either of the tissues. With prolonged TE (*B*), however, there are significant differences; a tissue with short T2 rapidly loses signal and rapidly becomes dark, while a tissue with a long T2 remains brighter for longer. (From: Weishaupt et al. 2006)

T1 and T2 relaxation are completely independent and proceed simultaneously.

Image Contrast

Various parameters of a tissue determine its brightness and thus the image contrast on the MR image. The proton density, the number of excitable spins per voxel, specifies the maximum signal that can be produced by a tissue. The T1 time of a tissue determines how quickly the spins of an excitation can recover and be excited again. The T2 time essentially determines how quickly the MR signal decays after excitation.

Proton density, T1, and T2 are specific characteristics that can be used to distinguish among different tissues.

Repetition Time

The repetition time (TR) significantly influences the T1 contrast. It is the time that elapses between two consecutive excitations of the same slice. The longer it lasts, the more the excited spins flip back into the Z direction and the more longitudinal magnetisation there is available in the next excitation.

If the TR is short (i.e. < 600 m/s), T1 can significantly influence the image contrast. Tissue with long T1 produces less signal than tissue with short T1 and also appears dark on the image.

If the repetition time is relatively long (i.e. > 1,500 m/s), all tissues, including those with long T1, have sufficient time to relax. The choice of repetition time can be determined with T1 weighting.

Echo Time and T2 Weighting

The echo time (TE) is the amount of time that is allowed to elapse between excitation and measurement of the MR signal. In the magnetic field, the gradient causes heterogeneities, which further amplify the T2 and T2* effects. The excited spins spiral out of phase and thus destroy the MR signal. Before each measurement, these de-phasing effects must first be reversed so that the spins are once again in phase.

The TE determines the influence that T2 has on the image contrast. T2 is much shorter than T1 and is in the range of up to a few 100 m/s. By choosing the TE, the T2-weighted image is determined. Tissues with short T2 produce little signal and appear dark on the MR image, while tissues with a long T2 appear bright.

Pulse Angle

A reduced pulse angle is used to obtain sufficient signal at a very short repetition time. The spins are no longer deflected by 90°, but rather only by 30°, for example. Less signal is obtained in the XY plane, but a portion of the magnetisation remains in the Z direction and is thus available for the next stimulation.

An "Ernst angle" refers to those pulse angles that yield the maximum signal for a given TR and TE.

Pre-Saturation

Another method of influencing the image contrast is pre-saturation. For this purpose, a 90° or 180° pulse is applied to the layer to be examined before the measurement begins. Pre-saturation can be applied for all of the base pulse sequences. The T1 contrast can be enhanced by the pre-saturation pulse. The shorter the time that elapses between the pulse and the start of the actual measurement, the stronger the effect. The strength of the T1 contrast can also be controlled by varying the distance between the 180° inversion pulse and the excitation pulse (= inversion time T1). The inversion time can be selected such that the magnetisation of the tissue at the excitation = 0 and hence the signal of a corresponding tissue disappears. In this way, the fat signal can be suppressed with a short T1, and the CSF signals can be suppressed with a long T1.

Transfer of Magnetisation

Water and fat molecules are relatively small and are highly mobile under *in vivo* conditions. Protons of macromolecules, e.g. proteins, have a wider range of Larmor frequencies than the protons of free water do. They can therefore be excited by radiofrequency pulses. This leads to saturation of the magnetisation of macromolecular protons, which in turn results in signal decay. This signal decay depends on the concentration of macro-molecules and on the interactions with free water. It is referred to as a transfer of magnetisation. The decay in signal intensity resulting from transfer of magnetisation is highly evident in solid tissues. However, the effect in liquids and adipose tissue is low.

The indirect effects of the exchange of the saturation of the magnetisation between free and bound protons can be measured. This is called a magnetisation transfer contrast (MTC) (Fig. 5.3). This technique is used in the imaging of cartilage in order to improve the contrast between synovial fluid and cartilage. The technique is based on the fact that synovial fluid has few bound protons while cartilage has a large proportion of bound protons. To a large extent, this manifests as a transfer of magnetisation. In the CNS, gadolinium-enriching lesions (e.g. in multiple sclerosis) can be better detected using the magnetisation transfer contrast.

Selection of Layers and Spatial Encoding

In order to be able use the MR signals for imaging, they must be spatially encoded. MRI is a tomographic method, i.e. sectional

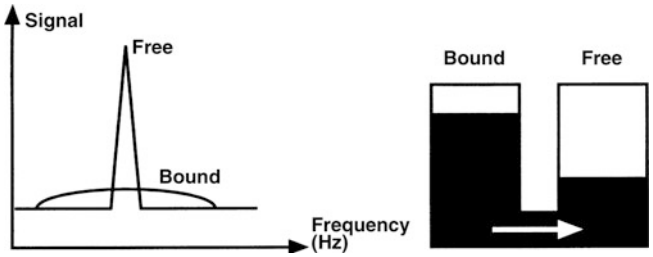

Fig. 5.3 Schematic representation of the magnetisation transfer contrast. (From: Weishaupt et al. 2006)

images of the body are generated. To selectively excite a section, the magnetic field along the Z direction is made heterogeneous in the Z direction. An additional solenoid amplifies or attenuates the magnetic field to varying degrees. The magnetic field now has a gradient in the Z-direction. This means that the Larmor frequency in the Z-direction is different; each section now has its own frequency. With a certain frequency, a corresponding layer can be accurately excited (Fig. 5.4).

Slice thickness and position are determined by the slice gradient. Because the desired gradient length can be selected, MR sectional images can be produced in any orientation. The spatial coding can be broken down into a phase and frequency encoding. To encode a phase, a gradient in the Y direction (phase gradient) is activated following excitement. This results in a phase shift of the spins against each other. This depends on the duration and strength of the phase encoding gradient as well as the location. After a certain time, the gradient is switched off again. All spins precess as fast as they did before being excited. However, the phase advance (i.e. the phase shift) remains. Each row within the slice can thus be identified through each phase. Frequency encoding is done in the second direction, i.e. the X direction. The frequency gradient causes the magnetic field to increase from right to left, and the Larmor frequencies behave accordingly. If the MR signal is measured, the entire frequency spectrum is received. Each volume element (voxel) is clearly characterised by frequency and phase.

Phase and frequency formally contain identical information. The quotient of the phase angle and the gradient duration (t) gives the precision frequency up to a factor of 2 π. Consequently, the spatial information underlying the phase can be reconstructed via Fourier transformation if the measuring sequence is repeated while the duration of the phase-encoding gradient is incremented. Alternatively, the gradient can be incremented. Overall, during imaging, spatially coded time signals are recorded as a function of gradient duration and strength. A two-dimensional raw-data matrix corresponds to such a grid of n rows and nF columns, which are filled in the course of the frequency or phase encoding. The actual image is calculated by Fourier transformation.

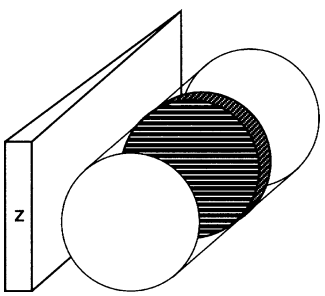

Fig. 5.4 Slice selection by the Z gradient. At a specific frequency, precisely one specific slice (*hatched*) is excited. The adjacent layers have different resonant frequencies and are not affected. (From: Weishaupt et al. 2006)

Like a hologram, the K-space contains information about the entire image and does not simply correspond to a point on the image matrix.

Figure 5.5 shows a schematic representation of the raw data in the K-space. The central lines in the K-space most strongly determine the contrast, while the outer lines mainly determine the spatial resolution.

It is sometimes advantageous to examine a whole volume at once rather than measuring only a number of individual slices. When measuring, the spatial information must be obtained via the direct direction (Z).

A Fourier transformation must now be performed in the Z direction in addition to the X and Y directions. The result is a three-dimensional set of data from the seamless volume from which reconstructions and projections can be calculated as desired.

Determinants of the Signal-to-Noise Ratio

The interaction between the MR signal and the magnitude of the noise is expressed as a signal-to-noise ratio (SNR). Mathematically, the SNR consists of the quotient between the signal intensity of an region of interest (ROI) divided by the standard deviation of the signal intensity of an area outside of the imaged body part or object.

The SNR is determined by the following parameters:

- Slice thickness and bandwidth
- Field of view
- Size of the image matrix
- Number of measurements
- Image parameters (TR, TE, flip angle)
- Magnetic field strength
- Selection of transmitting and receiving coil (RF coil)

Resolution of Signal/Noise Ratio, Measurement Time

The resolution of an MR image is determined by the slice thickness, pixel dimensions, and finally the quotient of the field of view and matrix size. For three-dimensional blocks, the measurement volume is composed of a sequence of partitions. In two-dimensional imaging, the distance between adjacent layers can be adjusted as well. In general, the smaller the voxel size, the greater the resolution of the MR image.

For optimal image resolution, the layers should be as thin as possible with a high SNR. However, thinner slices are associated with more noise. Conversely, thicker slices are associated with an increase in the SNR.

The bandwidth is the spectrum of the spin frequencies that detects an MR system at the frequency encoding. A high bandwidth allows faster data acquisition and has a reduced susceptibility to chemical-shift artefacts. Halving the bandwidth results in an improvement of the SNR by approximately 30%.

The inter-slice space (gap) is the distance between two slices. Ideally, there is no distance between the individual slices. However, this is not possible in spin-echo sequences. The sinusoidal RF profile of spin-echo sequences results in two immediately adjacent slices influencing each other, thereby leading to a decrease

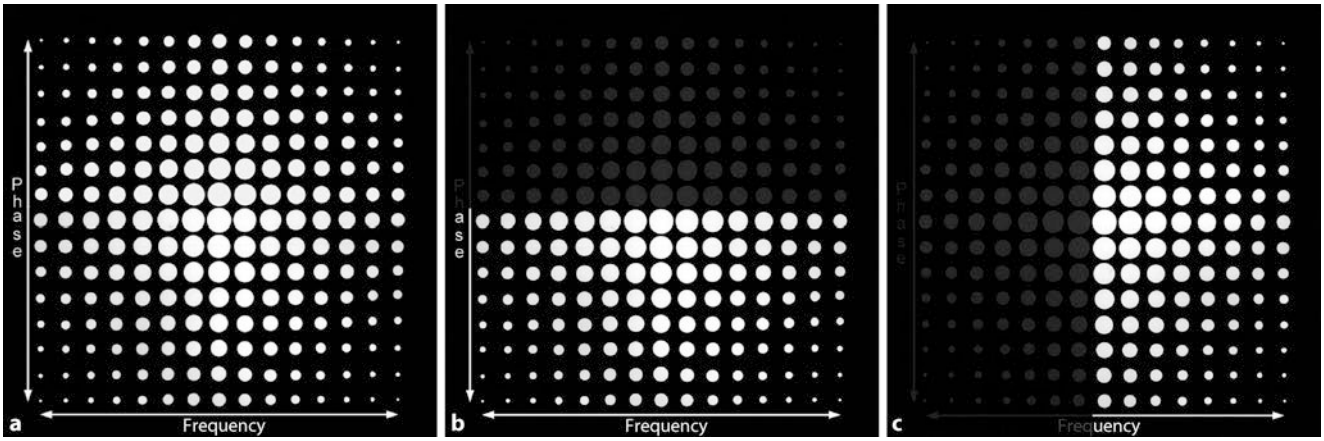

Fig. 5.5a–c **a** Graphical depiction for complex K-space acquisition. Each pixel represents a K-space line in frequency and phase direction. **b** Graphical depiction of the "partial Fourier technique". Slightly less than half of the K-lines in the phase direction are not collected (*grey dots*). These are filled by mathematical interpolation. **c** Graphical depiction of the "fractional echo technique". Slightly less than half of the K-space is not directly filled (*grey dots*). The unfilled portions correspond to the partial echoes that were not measured. The resulting image will have a resolution similar to that of **b**. However, the signal-to-noise ratio will be lower (less "real" data). (From: Weishaupt et al. 2006)

in the SNR. By using an intermediate slice spacing, this partial excitation from adjacent slices is minimised (typically 25–50% of the slice thickness).

There is a close relationship between field of view and SNR; for a given matrix size, the field of view determines the pixel size. The smaller the voxel, the lower the SNR. The image acquisition time is directly proportional to the matrix size. A higher spatial resolution in a reasonable time can be achieved by only reducing the field of view in the phase direction (rectangular field of view). Because the spatial resolution is determined by the matrix size in the frequency direction and the image acquisition time is determined by the matrix size in the phase direction, the matrix can be reduced in the phase direction without lowering the spatial resolution. In a "rectangular field of view", only half of the K lines in the direction of the phase are collected in the K-space.

Another way to decrease image acquisition time without affecting the voxel size is to incompletely scan the K-space (**partial Fourier technique**). The remaining K-space is mathematically interpolated (Fig. 5.5b). This leads to a reduction in the measurement time as well as a reduction of the SNR.

The number of measurements (number of excitations) is the number of times the signal of a particular slice is measured. Increasing the number of measurements increases the SNR.

Sequence type, TE, TR, and the flip angle also affect the SNR. The longer the TR, the higher the SNR. The longer TE, the lower the SNR.

At higher magnetic field strengths, the longitudinal magnetisation increases because more protons align along the main axis of the magnetic field. The SNR is thereby increased.

Pulse Sequences

Spin Echo Sequences

The spin-echo sequence is characterised by excitation with a slice-selective 90° RF pulse (Fig. 5.6). The transverse magnetisation then decays with T2*. After one half of the desired response time has elapsed, a 180° pulse is transmitted, which reverses the order of the spins. The advantage of the spin-echo sequence is its insensitivity to static field heterogeneities as well as the very good image quality that results. The disadvantage is the relatively long measurement time and thus a greater sensitivity to motion artefacts.

Multi-Slice Imaging

In multi-slice imaging, this time is used between two excitations in order to excite additional slices (Fig. 5.7). One disadvantage of this technique is that protons are excited outside the desired slice as a result of imperfections of the slice profile or imperfections of the RF pulse sequence. This leads to a decrease in the longitudinal magnetisation and can reduce the signal.

Inversion Recovery Sequence

The inversion recovery sequences are used to acquire T1-weighted or fat suppressed images. These are spin-echo sequences preceded by a 180° pulse. In contrast to the spin-echo sequences, in an IR sequence, a 180° pulse is first transmitted. This reverses the longitudinal magnetisation from the positive Z direction to the negative Z direction (Fig. 5.8). The relaxation of the longitudinal magnetisation vector proceeds through the transverse level to its original direction. After a period of relaxation, the initial pulse of the spin echo sequence is radiated. The time between the radiation of the 180° pulse and the 90° pulse is referred to as the inversion time (TI). The image contrast can be changed in order to change the inversion time.

In clinical routine, two inversion recovery sequences are primarily applied:

- Short inversion time inversion recovery sequence (STIR)
- Fluid-attenuated inversion recovery sequence (FLAIR)

The **STIR sequence** is frequently used for fat suppression. Here, fat can be reliably suppressed. The inversion time is chosen such that the 90° pulse is sent at the point in time at which the T1 relaxation curve has a zero crossing for fat. The fat signal is thereby suppressed. For a field strength of 1.5 Tesla, the required TI time